

Title	Thermodynamic Studies on the Krafft point in Aqueous Surfactant Systems
Author(s)	Tsujii, Kaoru
Citation	大阪大学, 1983, 博士論文
Version Type	VoR
URL	https://hdl.handle.net/11094/24327
rights	
Note	

Osaka University Knowledge Archive : OUKA

<https://ir.library.osaka-u.ac.jp/>

Osaka University

Thermodynamic Studies on the Krafft Point
in Aqueous Surfactant Systems

by

Kaoru Tsujii

Tochigi Research Laboratories

Kao Corporation

Contents

General Introduction and A Historical Review	1
--	---

Part I

Krafft Points of Binary Surfactant Mixtures

Introduction	7
Experimental Section	8
Materials	8
Krafft-point Determinations	11
Differential Scanning Calorimetry	12
Composition Determinations of the Solid Phase in Binary Surfactant Mixtures	13
Detection of the Viscoelasticity	14
Infrared Absorption Spectra	14
Results	15
Krafft Point of Pure Surfactant	15
Krafft Point vs. Composition Curves of Binary Surfactant Mixtures	18
Composition of Surfactant Mixtures in Solid Phase	24
Infrared Absorption Spectra	30
Viscoelasticity of the Solution	30
Discussion	31
1. The Melting-point Model for Krafft Temperature	31

Qualitative Thermodynamic Descriptions for the Krafft-point Change based on the Melting-point Model	31
Eutectic System	32
System Displaying Complete Miscibility in the Solid Phase	34
System Displaying Addition-Compound Formation	37
2. Applicability of Anionic Surfactant in Hard Water	45

Part II

Krafft-point Depression of Some Zwitterionic Surfactants by Inorganic Salts

Introduction	49
Experimental Section	50
Materials	50
Krafft-point Determinations	50
Cmc Measurements	52
Differential Scanning Calorimetry	52
¹³ C-NMR Spectra	52
Results	52
Discussion	65
References	77
Acknowledgments	84

General Introduction and A Historical Review

Detergents may be the most famous and popular products in the practical applications of surface active agent (surfactant). The detergent, however, is the only one example of household products of surfactant. One can readily give the other examples of the products such as toiletry soaps, hair shampoos and rinses, fabric softeners, dish-washing detergents etc. The surfactants are also extensively used in many kinds of industries. They are now essential materials for various purposes in the fields of textile, pulp and paper, mining, cosmetic, food, painting, agricultural, pharmaceutical, rubber and plastics, building and construction and even petroleum and fuel industries. In such variety of surfactant applications, the emulsifying, foaming, wetting, adsorptive and solubilizing functions (surface activities in the wide sense) of the surfactants are utilized. Needless to say, these surface activities cannot be obtained without dissolution of the agents into water. The dissolution behaviors of the surfactant are, then, of great importance for practical applications of the agents.

The temperature-dependence of surfactant solubility into water is, interestingly, quite abnormal. Below a certain temperature called Krafft point, the solubility is considerably small (usually less than 1 wt %) as expected from the molecular structure of the

agent having a long hydrophobic hydrocarbon chain. Above the Krafft temperature, however, the solubility increases dramatically, and the mixture of surfactant and water becomes the homogeneous one phase in almost any composition ranges. Accordingly, we can safely say that the Krafft temperature governs the solubility of surfactant into water, and is one of the most important and basic quantities of the surfactant solutions together with the critical micelle (or micellization) concentration (cmc). However, the studies on the Krafft point itself have not yet been fully made, and the whole feature of the Krafft temperature is not still clearly given.

As understood from the term of Krafft point or Krafft temperature, the abnormal dissolution behavior of surfactant was discovered by F. Krafft and his co-workers.¹⁻³⁾ They found almost 90 years ago that, when cooled from a high temperature, the sodium soap solutions gave much amount of crystalline solid at a certain narrow temperature range depending slightly upon the concentration of the soap. They also pointed out that the above crystallization temperature was closely correlated with the melting point of the mother free fatty acid from which the soap was derived. The precipitated crystalline substance, however, was shown unexpectedly not to be the free fatty acid, but the sodium salt. The melting point of the dry sodium soap, on the other hand, was much higher than the crystallization-temperature mentioned above. Krafft could

not give any further insights for these discrepant results. After their papers reported, few attentions had been paid for long time to their work and also to the soap solution itself.⁴⁾

McBain and his collaborators found the micellar aggregates of soap molecules in 1913, which made an epoch in the surfactant chemistry.⁵⁻⁶⁾ Bury and co-workers followed them, and found similar micelle formation of butyric acid and potassium octanoate above a certain narrow range of concentration which was called "critical concentration for micelles".⁷⁻⁹⁾ They interpreted this phenomenon by the law of mass action; when the simple and associated molecules are in equilibrium, the colligative properties of the solution must change abruptly with increasing concentration, if the number of association is sufficiently large. They explained their data of freezing-points and partial specific volumes by this theory.⁷⁻⁸⁾ These new concepts, i.e., the micellar aggregates of soap molecules and the critical concentration for micelles, were reasonably taken into consideration by Murray and Hartley in order to account for the anomalous solubility-temperature curve of the hexadecylsulfonic acid and its alkali salts.¹⁰⁾ They said in their paper¹⁰⁾ "If the concentration of the non-aggregated form in equilibrium with the solid increases steadily in the usual way with increasing temperature, then as, after a fairly definite critical concentration is reached, the ratio of micellar to non-micellar form increases very rapidly, we shall have the effect of a very rapid

increase of total solubility with increasing temperature once a certain temperature is reached. This explanation, which is also suggested by Lottermoser and Püschel¹¹⁾, shifts the responsibility for the anomaly from the temperature to the concentration, the sharp rise of solubility occurring at a certain temperature only because it is at this temperature that a certain concentration is reached." This explanation for the abnormal solubility of surfactant was quite reasonable, and the idea of the Krafft point as a melting or crystallization temperature was abandoned. After Murray and Hartley, many authors followed their opinion for long time.¹²⁻¹⁷⁾

Shinoda and Hutchinson proposed the new pseud-phase separation model for micelles in 1962.¹⁸⁾ They regarded the micelle as a kind of phase of liquid state. Once this model was accepted, the Krafft point was necessarily considered again as the melting point of the surfactant in aqueous solutions, since the solid agent was in equilibrium with and transformed into the liquid (micellar) phase at the Krafft temperature. The discrepant result observed by Krafft, namely, much difference between the melting point of dry surfactant and the Krafft point in water was solved by considering the hydration effect of the hydrophilic head group upon the melting temperature of surfactant, as noticed previously by Lawrence.¹⁹⁾ Sodium acetate in the anhydrous state melts at 319°C but, when hydrated with 3 molecules of water, melts at 58°C. This may be the

case, he thinks, also in the melting (Krafft) point of the surfactant.¹⁹⁾ The surfactant crystals were indeed found to be the hydrated ones in several cases.^{11, 13, 16, 20-21)} The liquid-like nature of the micellar state was also substantiated by several experimental means,²²⁻³²⁾ and now widely believed.³³⁻⁴⁰⁾ Shinoda and co-workers extended the melting-point model for Krafft temperature to some surfactant⁴¹⁻⁴⁷⁾ and mixed surfactant systems.⁴⁸⁻⁵⁰⁾ No one else, however, has fully accepted this model, since the Murray and Hartley's explanation is not necessarily denied by this model.

The melting-point model for Krafft temperature gives us some useful insights to depress the Krafft point and dissolve an important surfactant into water. The opinion of Murray and Hartley, on the other hand, is just the explanation for the phenomenon, and does not give any contributions to the above purposes. Accordingly, from the practical point of view, the melting-point model is much better one if it is true. The experimental evidences given so far which support the melting-point model are as follows:

- (1) The partial molal volume changes of sodium alkylsulfates and sulfonates at their Krafft points are close to the molal volume changes of analogous paraffin chain compounds at their melting points.²⁷⁾
- (2) For a homologous series of sodium n-alkylsulfates, their Krafft points show a pronounced alternating between the

odd-carbon-numbered and the even-numbered surfactants,⁵¹⁾ similarly to the well-known nature in the melting points of long chain compounds such as paraffins, alkylamines and fatty acids.⁵²⁾

- (3) The Krafft point of a surfactant is depressed when an organic compound is solubilized into the micelle⁴⁸⁾ or another surfactant is mixed,⁴⁹⁻⁵⁰⁾ just like the freezing-point depression phenomena of ordinary substances.

In the present work, some novel phenomena on the Krafft points of binary surfactant mixtures and zwitterionic surfactants have been found, and shown to be the new evidences for the melting-point model of the Krafft point. In Part I, the Krafft point vs. composition curves of binary surfactant mixtures will be discussed, in connection with the applicability of anionic surfactants in hard water. A novel Krafft-point depression phenomenon of some zwitterionic surfactants by inorganic salts will be argued thermodynamically in Part II.

Part I

Krafft Points of Binary Surfactant Mixtures

Introduction

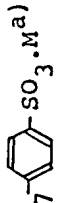
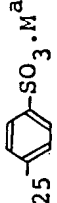
The Krafft point vs. composition curves of binary surfactant mixtures may give one of the most useful thermodynamic evidences to confirm the melting-point model. If the similar diagrams to the melting point vs. composition curves of binary mixtures of ordinary substances are observed also in the Krafft points of mixed surfactant systems, the melting-point model will be strongly supported. A purpose of this part is to present some examples of the above.

Another purpose in Part I is to examine the applicability of anionic surfactants in hard water from the standpoint of practical applications of the agents. The Krafft points of calcium salts of ordinary anionic surfactants are generally higher than ambient temperature, and they cannot be used in hard water without any sequestering agents. The phosphate builders are well-known to be the most commonly used sequestering agents in detergent formulations but are now implicated in eutrophication problems in some developed countries. It is then of great importance for practical uses of surfactants to find the agent which is applicable in hard water. In line with this interest, the Krafft points of the sodium and calcium salts of anionic surfactants and their mixtures have been measured to examine their applicability in hard water.

Experimental Section

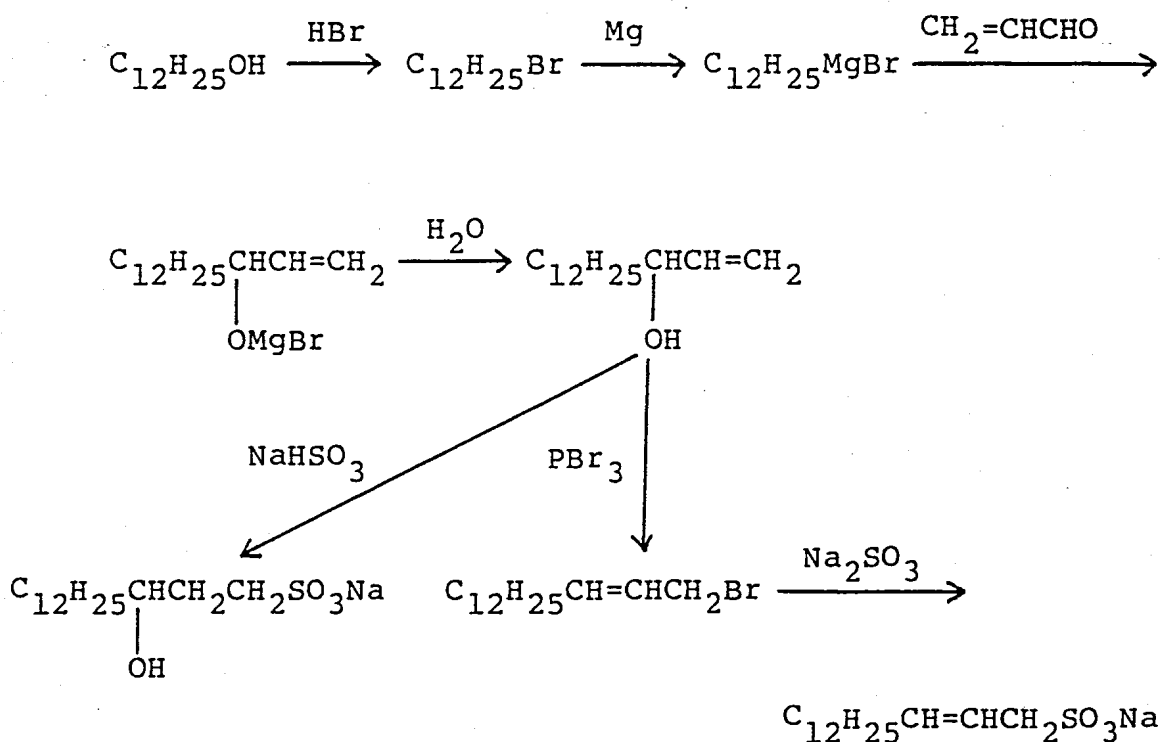
Materials. All surfactant samples used in Part I and their abbreviations are listed in Table I. Almost all samples were synthesized in Wakayama Research Laboratories of Kao Corporation, and the procedures of their preparations will be described below briefly. $R_{12}SO_4Na$ was synthesized by ordinary $ClSO_3H$ sulfation of dodecylalcohol (99% pure by gas chromatography) obtained from Tokyo Kasei Ltd. Sodium and calcium dodecylmono- and tris(oxyethylene)sulfates were prepared by essentially the same procedures described by Hato and Shinoda.⁵⁰⁾ The starting mono- and tris(oxyethylene)dodecyl ether purchased from Nikko Chemicals Co. were shown to be more than 98% pure by gas chromatography. Sodium and calcium salts of the final products were purified by repeated recrystallization from 2-propanol/ethanol mixture (3/1 by volume). Other sodium alkylpoly(oxyalkylene)sulfates with polydisperse oxyalkylene units were synthesized by the same manner mentioned above. Most of these ether sulfates could not be recrystallized because of their paste-like nature. Sodium octyl- and dodecylbenzenesulfonates were synthesized by $ClSO_3H$ sulfonation of 1-phenyl-n-octane and 1-phenyl-n-dodecane (99% pure by gas chromatography) purchased from Tokyo Kasei Ltd. After neutralization with NaOH, the crude surfactants were recrystallized twice from ethanol. The corresponding calcium salts of the above

Table 1: Surfactant samples used in Part I and their abbreviations

Name of surfactant	Molecular structure	Abbreviation
Sodium dodecyl sulfate	$n\text{-C}_{12}\text{H}_{25}\text{OSO}_3\text{Na}$	$R_{12}\text{SO}_4\text{Na}$
Alkyl poly(oxyethylene)sulfates	$n\text{-C}_n\text{H}_{2n+1}\text{O}(\text{CH}_2\text{CH}_2\text{O})_q\text{SO}_3\cdot\text{M}^a)$	$R_n(\text{OE})_q\text{SO}_4\cdot\text{M}^a)$
Alkyl poly(oxypropylene)sulfates	$n\text{-C}_n\text{H}_{2n+1}\text{O}(\text{CH}_2\text{CHO})_p\text{SO}_3\cdot\text{Na}$ CH_3	$R_n(\text{OP})_p\text{SO}_4\text{Na}$
Octylbenzene sulfonates	$n\text{-C}_8\text{H}_{17}$ 	$R_8\phi\text{SO}_3\cdot\text{M}^a)$
Dodecylbenzene sulfonates	$n\text{-C}_{12}\text{H}_{25}$ 	$R_{12}\phi\text{SO}_3\cdot\text{M}^a)$
Sodium tetradecane-1-sulfonate	$n\text{-C}_{14}\text{H}_{29}\text{SO}_3\text{Na}$	$R_{14}\text{SO}_3\text{Na}$
3-Hydroxypentadecane-1-sulfonates	$n\text{-C}_{12}\text{H}_{25}\text{CH}(\text{OH})\text{CH}_2\text{CH}_2\text{SO}_3\cdot\text{M}^a)$	$R_{15}(\text{OH})\text{SO}_3\cdot\text{M}^a)$
2-Pentadecene-1-sulfonates	$n\text{-C}_{12}\text{H}_{25}\text{CH}=\text{CHCH}_2\text{SO}_3\cdot\text{M}^a)$	$R_{15}(\text{C}=\text{C})\text{SO}_3\cdot\text{M}^a)$
N,N-Dimethyl-N-carboxymethyl alkylammonium inner salt	$n\text{-C}_n\text{H}_{2n+1}\overset{\dagger}{\text{N}}(\text{CH}_3)_2\text{CH}_2\text{COO}^-$	$R_n\text{DMCMA}$
N,N-Dimethyl-N-(3-sulfopropyl) alkylammonium inner salt	$n\text{-C}_n\text{H}_{2n+1}\overset{\dagger}{\text{N}}(\text{CH}_3)_2\text{CH}_2\text{CH}_2\text{SO}_3^-$	$R_n\text{DMSPA}$
N,N-Dimethylalkylamine oxide	$n\text{-C}_n\text{H}_{2n+1}\text{N}(\text{CH}_3)_2\text{O}$	$R_n\text{DMAO}$
Dodecanoyldiethanol amide	$n\text{-C}_{11}\text{H}_{23}\text{CON}(\text{CH}_2\text{CH}_2\text{OH})_2$	$R_{12}\text{DEA}$

a) M = Na or 1/2Ca

alkylbenzenesulfonates were prepared by metathesis in aqueous CaCl_2 solutions and recrystallized from ethanol. $\text{R}_{14}\text{SO}_3\text{Na}$ was synthesized by the reaction of 1-bromotetradecane with NaHSO_3 (Strecker's reaction) in an autoclave, and purified by the repeated recrystallization from water/ethanol mixture (=4/1 by volume). The starting 1-bromotetradecane was obtained from Tokyo Kasei Ltd., and shown to be more than 95% pure by gas chromatography. Sodium 3-hydroxypentadecane-1-sulfonate and sodium 2-pentadecene-1-sulfonate which were the model compounds of α -olefin sulfonates were synthesized by the following procedures.^{53,54)}



The starting dodecanol was purified by distillation under reduced pressure and shown to be more than 99% pure by gas chromatography. The reaction product obtained in each step was checked by IR spectra and gas chromatography. The final products were recrystallized several times from ethanol/water mixture (4/1 by volume). The purified samples were checked by elementary analysis and IR and NMR spectra. The calcium salts of the above surfactants were prepared by metathesis in water and recrystallized by the same manner as the above. R_n DMCMA was prepared by ordinary carboxymethylation of N,N-dimethylalkylamine (98% pure) with sodium monochloroacetate in a water/ethanol mixture. The reaction product was recrystallized from methanol or benzene repeatedly after evaporation of the reaction solvent. R_{12} DMSPA were synthesized by the reaction of N,N-dimethylalkylamine with 1,3-propanesultone according to essentially the same procedures used by Fendler et al.⁵⁵⁾ R_n DMAO was prepared by H_2O_2 oxidation of N,N-dimethylalkylamine.^{56,57)} The crude product was recrystallized three times from an acetone/benzene mixture. R_{12} DEA was purchased from Kawaken Fine Chemicals Co. and used without further purification. Deionized and distilled water was used to prepare the sample solutions.

Krafft-Point Determinations. The Krafft point was determined from the solution temperature on gradual heating (at most

1°C/min.) under vigorous stirring.⁵⁰⁾ The solution temperature was observed photometrically or visually. In the photometric method, the transmittance of light through sample solutions and the temperature of the solution measured with a thermister were plotted on an X-Y recorder.⁵⁸⁾ The temperature at which the transmittance equalled that of pure water was taken as the Krafft point. The reproducibility of the Krafft point measured by both photometric and visual methods was within $\pm 0.3^\circ\text{C}$. When the Krafft point was above 80°C , the sample solutions were sealed in thick glass tubes after N_2 gas bubbling prior to heating. In order to obtain the hydrated solid agents equilibrated with their solutions, the samples were dissolved at high temperature and precipitated by cooling. Sometimes, the crystalline surfactant was not obtained by simple cooling at ca. 0°C because of supercooling. In such cases, the sample solutions were frozen and thawed repeatedly until the solid agents were precipitated.

Diferential Scanning Calorimetry. Differential scanning calorimetry (DSC) was performed with a Daini Seikosha Type SSC-544 DSC apparatus. The sample solution ($60\ \mu\text{L}$) was put in a sealed aluminum or silver cell and heated at the rate of $0.6^\circ\text{C}/\text{min}$. The concentration of the sample solutions was usually the same as that of the solutions used in the Krafft-point measurements. Repeated measurements (at least three times) of the transition enthalpy

agreed to within 5% of the mean. The DSC measurements could not be carried out at higher temperatures than 100°C because of the machine limitations.

Composition Determinations of the Solid Phase in Binary

Surfactant Mixtures. The aqueous solutions (150 mM) of binary surfactant mixtures with a given mixing ratio were maintained at a constant temperature below the Krafft point of the mixture. The precipitated solid phase in equilibrium with the solution was filtered quickly through a sintered glass disk. The composition of the collected solid surfactant was determined by the following methods.

Sodium and calcium ion contents were analyzed by flame photometry (Coleman, Model 21 flame photometer) to determine the solid-phase composition of the $R_{15}(OH)SO_3Na/R_{15}(OH)SO_3 \cdot 1/2Ca$ mixtures. Proton magnetic resonance (1H NMR) technique was employed to determine the composition of the $R_{15}(C=C)SO_3Na/R_{15}(OH)SO_3Na$ system. The collected solid agent was dissolved to be 10 wt % in deuterium oxide containing a small amount of sodium 2,2-dimethyl-2-silapentane-5-sulfonate (DSS) as an internal reference. 1H NMR measurements were carried out with a Varian Type EM-360L NMR spectrometer at 50°C. The contents of the $R_{15}(C=C)SO_3Na$ and $R_{15}(OH)SO_3Na$ were determined from the 1H NMR signal due to the protons of the double bond methine of

$R_{15}(C=C)SO_3Na$ (5.4-5.8 ppm from the DSS signal) and the methylene protons next to the sulfonate group of $R_{15}(OH)SO_3Na$ (2.7-3.1 ppm), respectively.⁵⁹⁾ The composition analysis of the $R_8\phi SO_3Na/R_{12}\phi SO_3Na$ system was made by means of high-speed liquid chromatography using a Merck RP-18 column. The solid sample was dissolved to be 10 mg/5 mL in a ethanol/water (3/1 by volume) mixed solvent. The sample solution (2 μ L) was injected and eluted with a methanol/water (4/1 by volume) mixed solvent containing 0.1 M sodium perchlorate. Each component of the mixture was detected by ultraviolet absorption at 225 nm.

Detection of the Viscoelastisity. Viscoelastisity of the mixed solutions of anionic and zwitterionic surfactants was detected by the simple method of swirling a sample solution and visually observing recoil of small air bubbles entrapped in the sample just after swirling was stopped.^{60,61)} The concentration of the sample solutions was the same as that of the solutions used in the Krafft-point measurements.

Infrared Absorption Spectra. Infrared absorption spectra of the solid $R_{12}SO_4Na$, $R_{12}DMCMA$ and their addition compound were observed with a Hitachi Model 260-50 infrared absorption spectrometer. The addition compound between both surfactants was obtained by quick filtration of the crystalline agent precipitated at

the temperature below its Krafft point, and dried in vacuo.

Results

The Krafft points of some of the surfactants used in this work (Part I and II) as a function of their concentration are listed in Table 2. The concentration dependence of the Krafft point is negligibly small in the narrow range of concentration above but close to their cmc. This result allows us to take the solution temperature at a certain concentration close to cmc as the Krafft point. Most of the Krafft points reported in this paper were determined in the way of the above.

Krafft Point of Pure Surfactant. The Krafft point of pure surfactant measured by both solution temperature and DSC curve are given in Table 3. The agreement between Krafft points from both methods is fairly good. It can be seen from the table that 1) among the anionic surfactants having the sulfate group as a hydrophilic head, their Krafft points decrease in the order of $R_nSO_4Na > R_n(OE)_qSO_4Na > R_n(OP)_pSO_4Na$,⁶²⁾ the same sequence of which is also observed by Weil et al^{63,64)}; 2) the calcium salts of alkylbenzenesulfonates show the surprisingly high Krafft points⁶⁵⁾; 3) the Krafft points of alkylpoly(oxyalkylene)

Table 2: Krafft temperatures of some surfactants as a function of their concentration

Surfactant	Medium	Krafft point /°C				
		0.5 mM	1.0 mM	1.5 mM	2.0 mM	5.0 mM
R ₁₆ ^{DMCMA}	pure water	11.9	11.9	12.1	12.1	
	0.1M NaCl		13.0	13.1	13.1	
R ₁₈ ^{DMCMA}	pure water	33.5	34.0	34.0	34.0	
	1.0M NaCl	34.5	34.4	34.6	34.6	
R ₁₈ ^{DMCPA}	pure water	24.0	24.0			24.0
	1.0M NaCl	18.5	19.0			19.2
R ₁₆ ^{DMSPA}	pure water	27.9	28.0	28.3	28.4	
	1.0M NaCl	24.4	24.4		24.2	
R ₁₈ ^{DMSPA}	pure water		73.4		73.4	
	1.0M NaCl	33.5	33.7	33.7	33.6	
R ₁₂ ^{CEA}	pure water				43.5	43.5
	1.0M NaCl		36.5	36.0	36.0	36.1

Table 3 : Krafft temperature of pure surfactant

Surfactant	Krafft temp. /°C	
	solution temp.	DSC
$R_{12}SO_4Na$	12.0, 16 ^{a)}	
$R_{12}(OE)SO_4Na$	9.0	8.5
$R_{12}(OE)_3SO_4Na$	< 0	
$R_{12}(OE)SO_4 \cdot 1/2Ca$	18.7	17.0
$R_{12}(OE)_3SO_4 \cdot 1/2Ca$	< 0	
$R_{12}(OP)SO_4Na$ ^{b)}	~ 0	
$R_{16}SO_4Na$	45 ^{a)}	
$R_{16}(OE)_3SO_4Na$ ^{b)}	35	
$R_{16}(OP)_3SO_4Na$ ^{b)}	28	
$R_{18}SO_4Na$	56 ^{a)}	
$R_{18}(OE)_3SO_4Na$ ^{b)}	49	
$R_{18}(OP)_3SO_4Na$ ^{b)}	41	
$R_8\phi SO_3Na$	26.0	25.5
$R_8\phi SO_3 \cdot 1/2Ca$	196.5	
$R_{12}\phi SO_3Na$	62.5	65.0
$R_{12}\phi SO_3 \cdot 1/2Ca$	269.0	
$R_{15}(OH)SO_3Na$	20.2	21.5
$R_{15}(OH)SO_3 \cdot 1/2Ca$	66.8	68.0
$R_{15}(C=C)SO_3Na$	35.5	40.0
$R_{15}(C=C)SO_3 \cdot 1/2Ca$	91.3	
$R_{16}DMSPA$	28.4	28.0

a) Data taken from reference 64.

b) The sample having polydisperse oxyalkylene units.

sulfates, on the other hand, are low enough to be used in cold and/or hard water.^{62,65)} These results are of special importance for practical uses of these surfactants, since the anionic surfactants applicable in hard water are now strongly required as mentioned previously.

Krafft Point vs. Composition Curves of Binary Surfactant

Mixtures. The Krafft point vs. composition curves observed in binary surfactant mixtures have been classified into three groups.^{62,65,66)} In group I, there exists a minimum in the Krafft point at a certain composition, whereas the Krafft point varies monotonously with changing composition in group II.⁶⁵⁾ The Krafft point vs. composition curves in group III are completely different from the above two cases, and show a maximum in the diagram.^{62,66)} The curves classified into groups II and III are observed for the first time by the present author and his collaborators.

Figures 1, 2, 3, and 4 show the Krafft point vs. composition curves which belong to the group I.⁶⁵⁾ In every binary system, one can see a minimum in the Krafft point at a certain composition. This same minimum has also been observed by Shinoda et al.^{49,50)} and Moroi et al.²¹⁾ in other surfactant systems. On the other hand, there appears no minimum point in the $R_8 \text{ SO}_3\text{Na}/R_{12} \text{ SO}_3\text{Na}$ system as shown in Figure 5.⁶⁵⁾ In this case, the Krafft point elevates monotonously with increasing mole fraction of $R_{12} \text{ SO}_3\text{Na}$

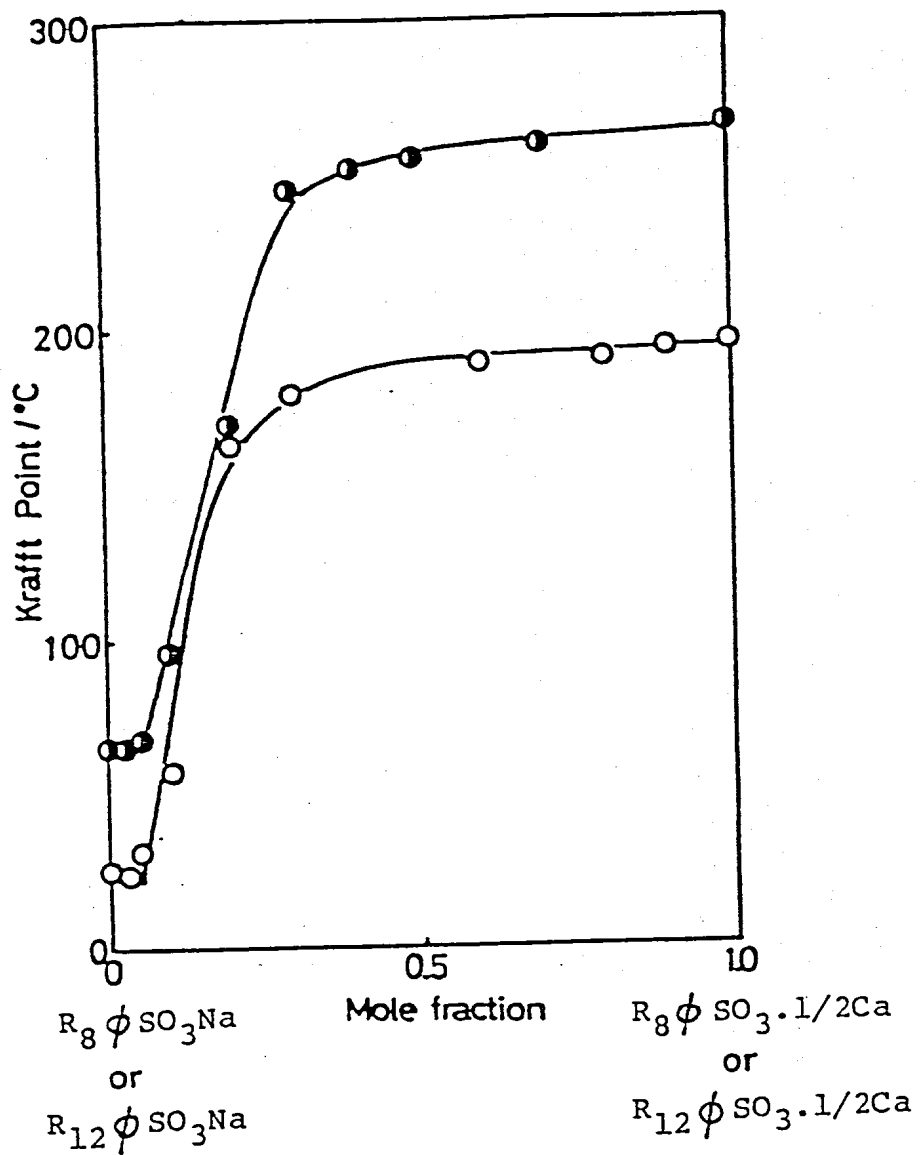


Figure 1. The Kraftt point vs. composition curves of the $R_8\phi SO_3Na/R_8\phi SO_3 \cdot 1/2Ca$ (○) and $R_{12}\phi SO_3Na/R_{12}\phi SO_3 \cdot 1/2Ca$ (●) systems.

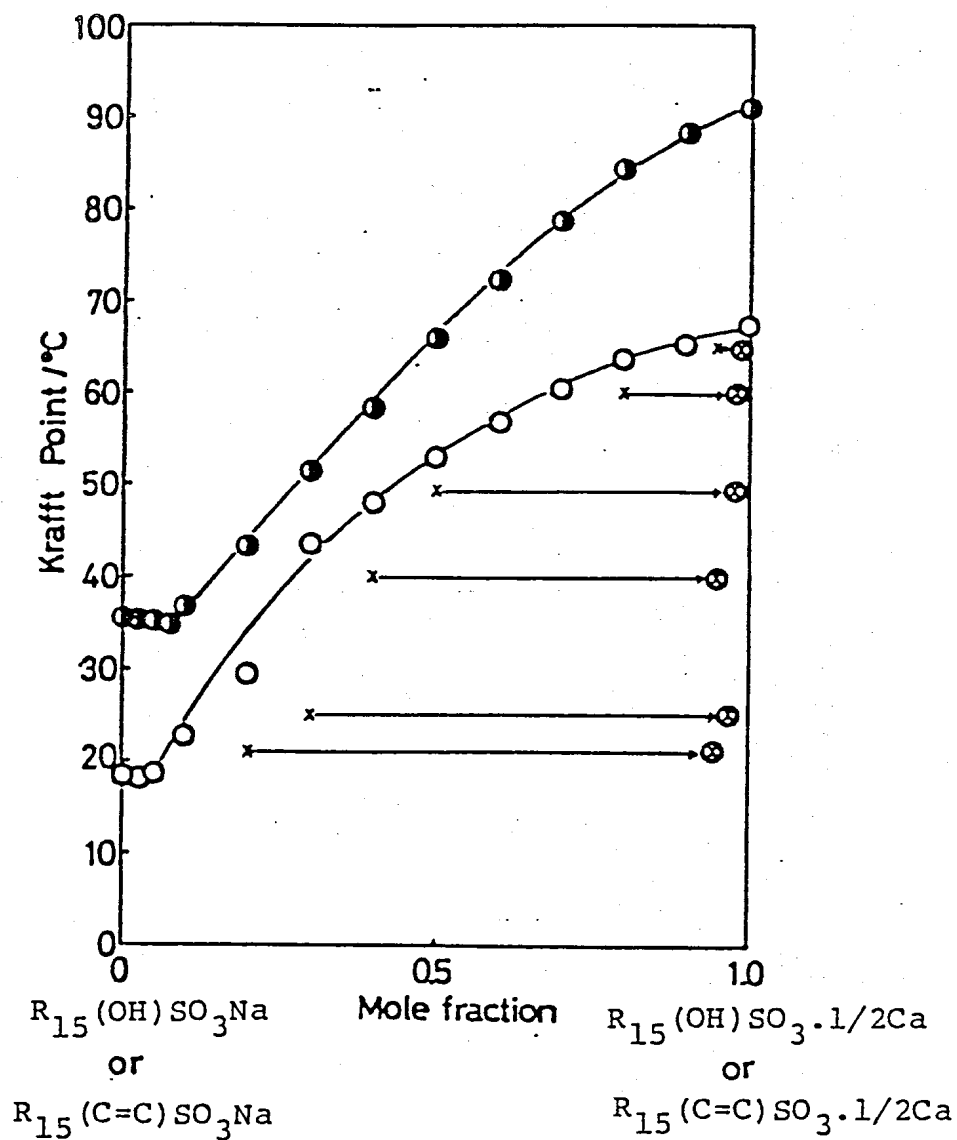


Figure 2. The Krafft point vs. composition curves of the $R_{15}(\text{OH})\text{SO}_3\text{Na}/R_{15}(\text{OH})\text{SO}_3 \cdot 1/2\text{Ca}$ (○) and $R_{15}(\text{C}=\text{C})\text{SO}_3\text{Na}/R_{15}(\text{C}=\text{C})\text{SO}_3 \cdot 1/2\text{Ca}$ (●) systems. The ⊗ marks indicate the composition of the $R_{15}(\text{OH})\text{SO}_3\text{Na}/R_{15}(\text{OH})\text{SO}_3 \cdot 1/2\text{Ca}$ mixtures in the solid phase collected at the given temperatures and mixing ratios marked with X signs.

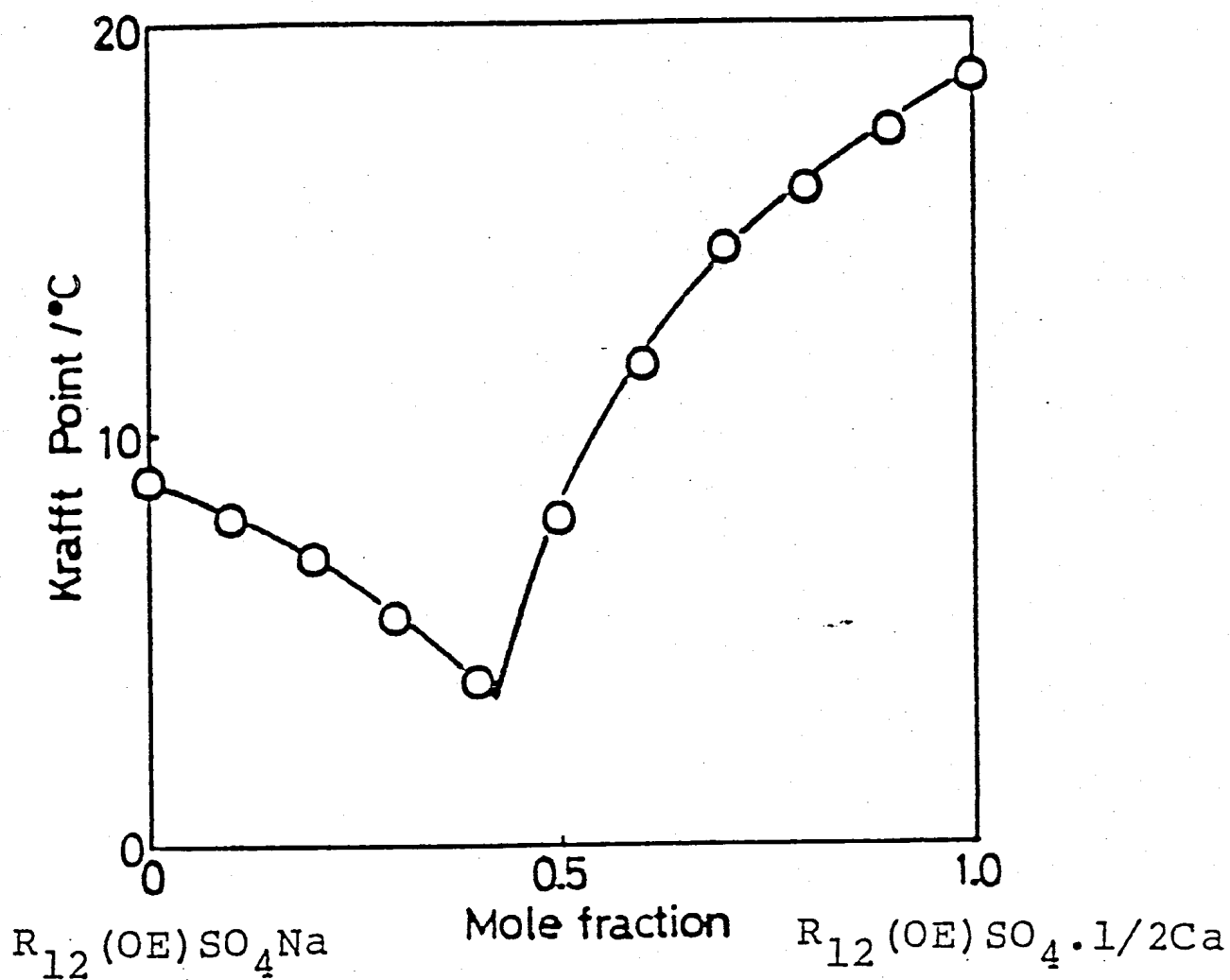


Figure 3. The Krafft point vs. composition curve of the $R_{12}(OE)SO_4Na/R_{12}(OE)SO_4 \cdot 1/2Ca$ system.

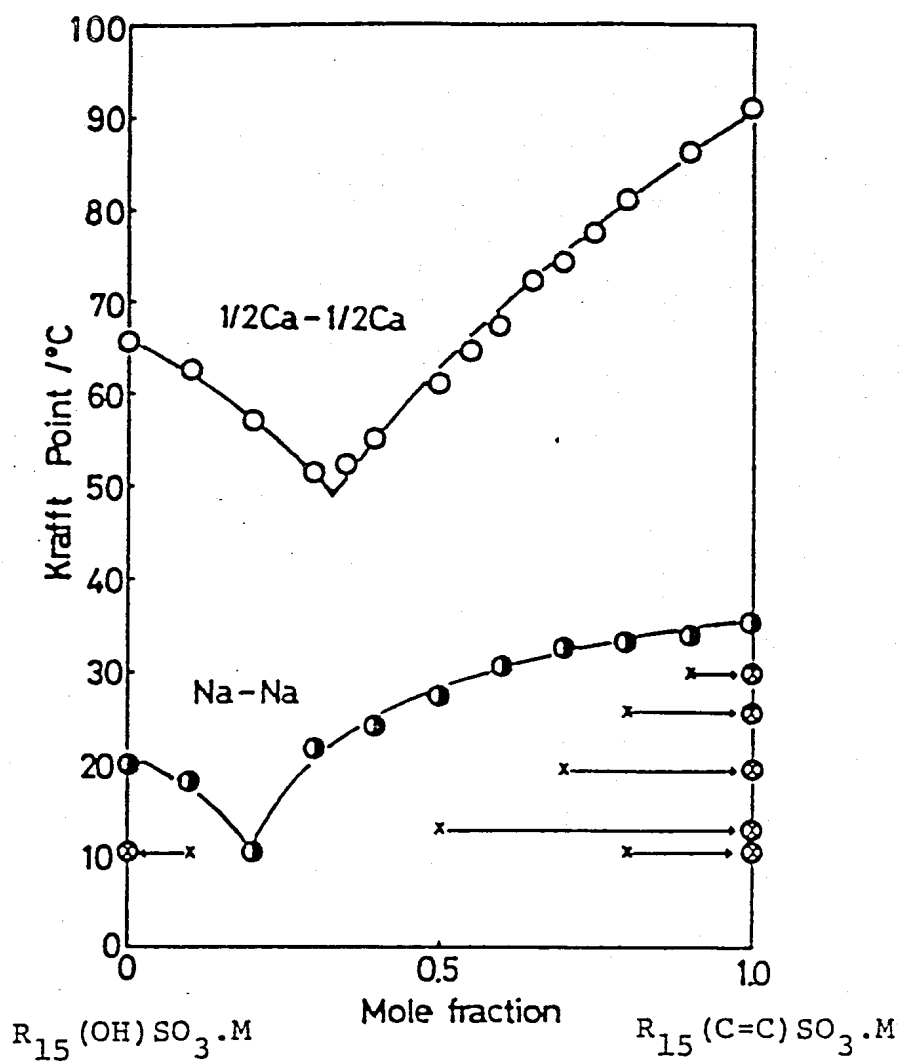


Figure 4. The Krafft point vs. composition curves of the $R_{15}(\text{OH})\text{SO}_3\text{Na}/R_{15}(\text{C}=\text{C})\text{SO}_3\text{Na}$ (●) and $R_{15}(\text{OH})\text{SO}_3\text{1/2Ca}/R_{15}(\text{C}=\text{C})\text{SO}_3\text{1/2Ca}$ (○) systems. The signs ⊗ and X have the same meanings as those described in the legend of Figure 2.

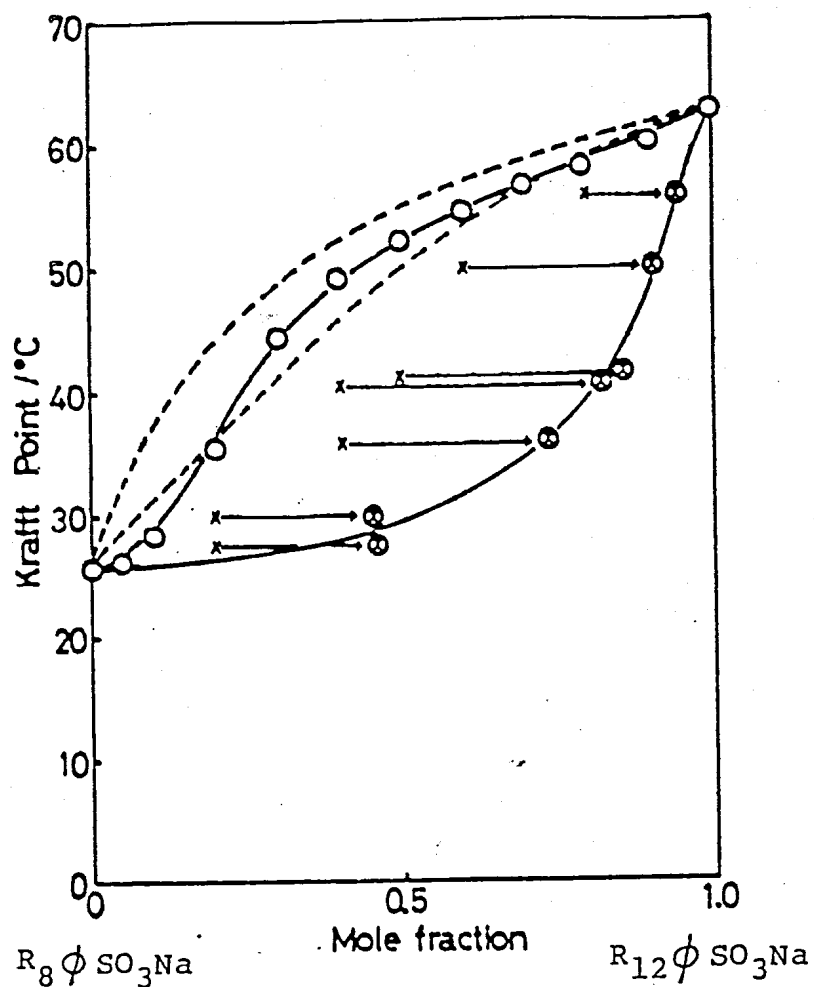


Figure 5. The Krafft point vs. composition curve of the $R_8\phi SO_3Na/R_{12}\phi SO_3Na$ system (O). The signs ⊗ and X have the same meanings as those described in the legend of Figure 2. The calculated liquidus (Krafft point) and solidus curves are shown by dotted lines.

(group II). All binary systems that show a maximum in the Krafft point vs. composition curves are the mixtures of anionic and zwitterionic surfactants (Figures 6-9).⁶⁶⁾ Such Krafft-point maximum has never been observed so far in any other surfactant mixtures, and can be ascribed to the addition-compound formation between both surfactants as discussed later. In the $R_{12}SO_4Na/R_{18}DMCMA$ system (Fig. 9), two kinds of Krafft point curve are observed. The hydrated crystalline phase which has lower Krafft point is, of course, metastable one. The Krafft point vs. composition curves of the $R_{12}SO_4Na/$, and $R_{14}SO_3Na/R_{12}DEA$ systems are shown in Figure 10. In these systems, there appears only one minimum point without any maxima.

Composition of Surfactant Mixtures in Solid Phase. The

compositions in the solid phase of the $R_{15}(OH)SO_3Na/R_{15}(OH)SO_3 \cdot 1/2Ca$, $R_{15}(OH)SO_3Na/R_{15}(C=C)SO_3Na$ and $R_8\phi SO_3Na/R_{12}\phi SO_3Na$ systems are shown in Figures 2, 4, and 5, respectively. In these figures, the compositions of the solid agents are indicated by the \otimes marks. These solid samples were collected at given temperatures below the Krafft points and mixing ratios marked by the \times signs. It is evident from these figures that, in the surfactant mixture which has a minimum point in the Krafft point vs. composition curve, the solid phase is composed of virtually a pure compound, whereas, with the

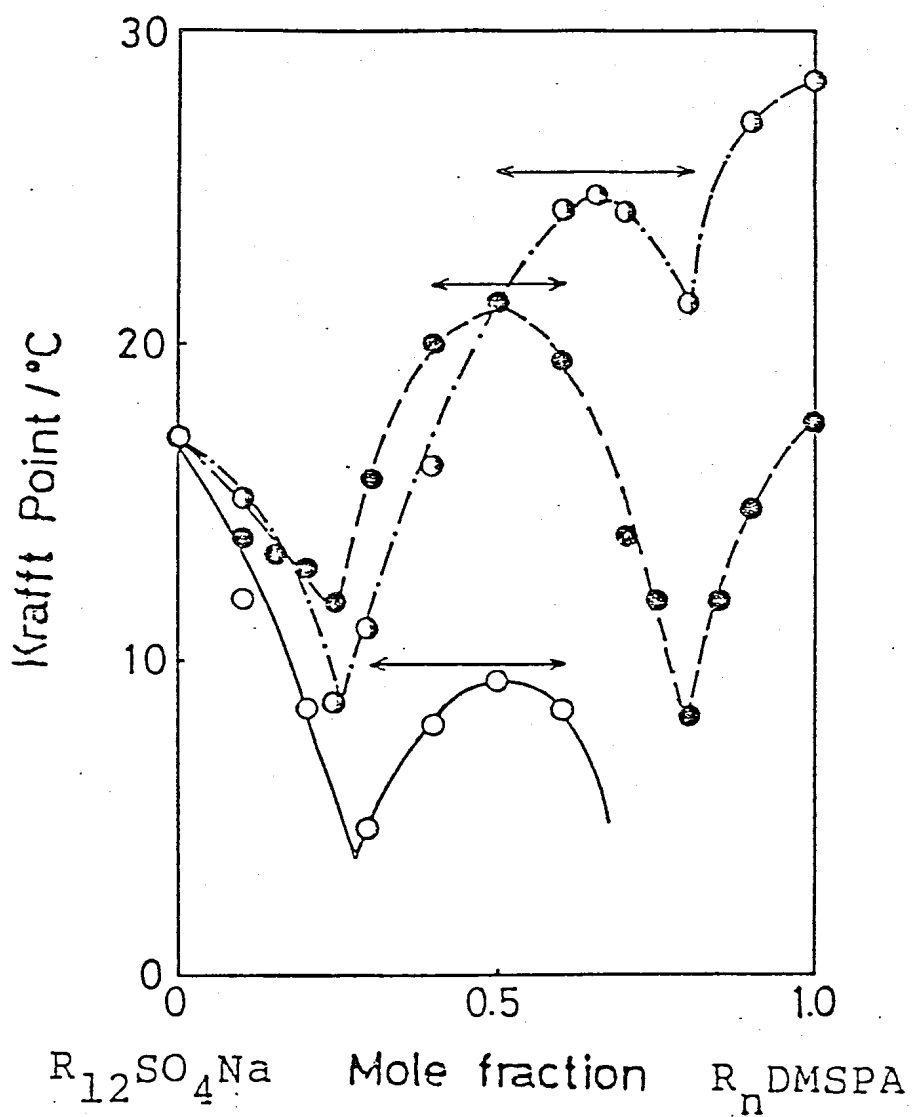


Figure 6. The Krafft point vs. composition curves of the $R_{12}SO_4Na/R_{12}DMSPA$ (\bigcirc), $/R_{14}DMSPA$ (\odot) and $/R_{16}DMSPA$ (\otimes) systems. The arrows (\longleftrightarrow) indicate the viscoelastic composition ranges in micellar solution phases for the above three systems.

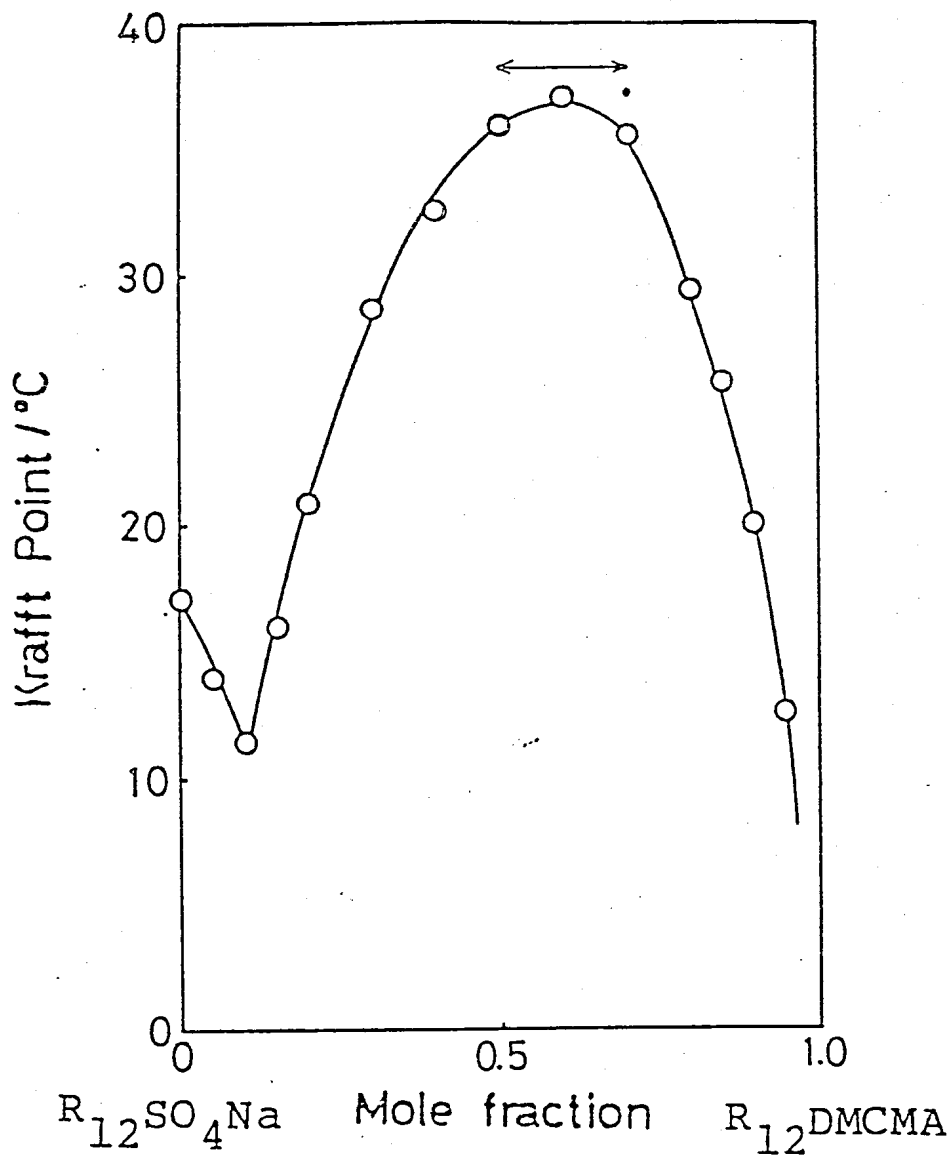


Figure 7. The Krafft point vs. composition curve of $R_{12}SO_4Na/R_{12}DMCMA$ system. The arrow has the same meaning as that described in the legend of Figure 6.

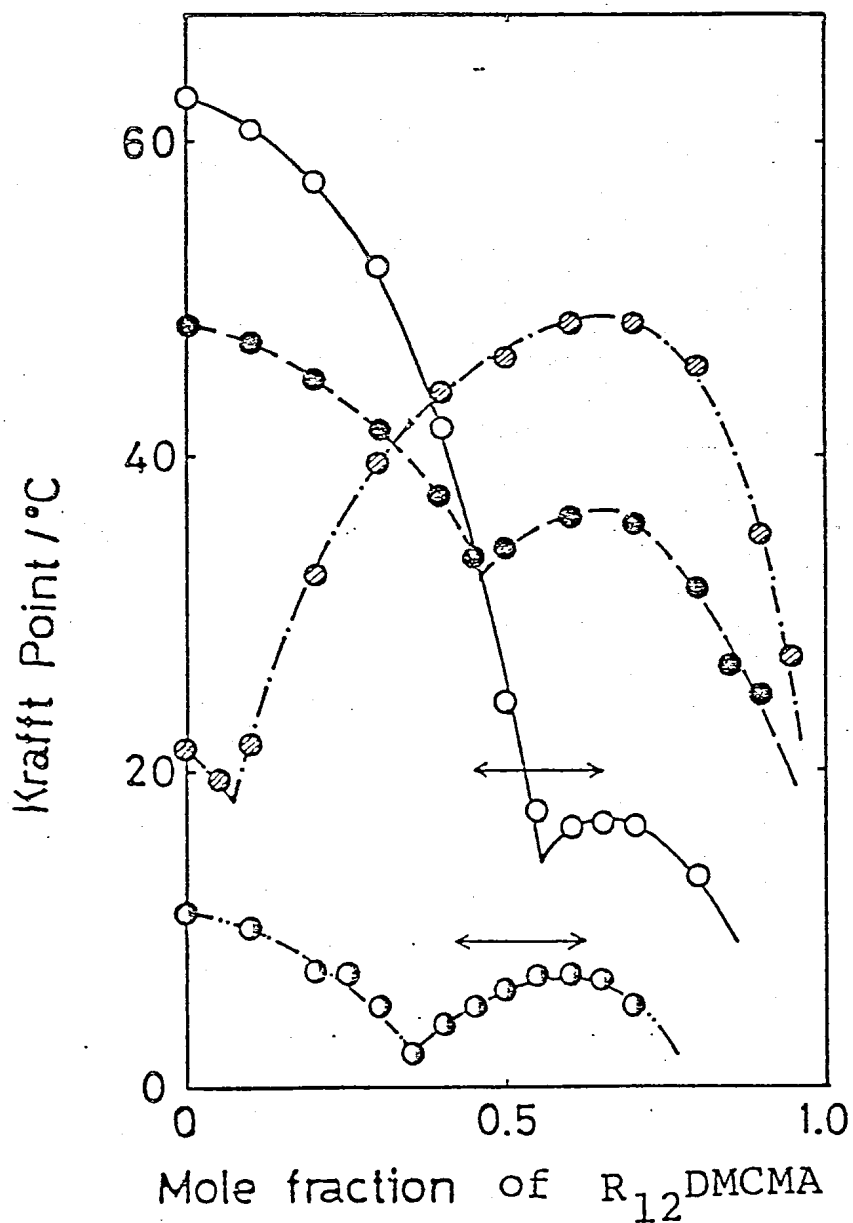


Figure 8. The Krafft point vs. composition curves of the $R_{14}SO_3Na/$ (●), $R_{15}(OH)SO_3Na/$ (⊙), $R_{12}(OE)SO_4Na/$ (⊗) and $R_{12}\phi SO_3Na/R_{12}DMCMA$ (○) systems. The arrows have the same meanings as those described in the legend of Figure 6.

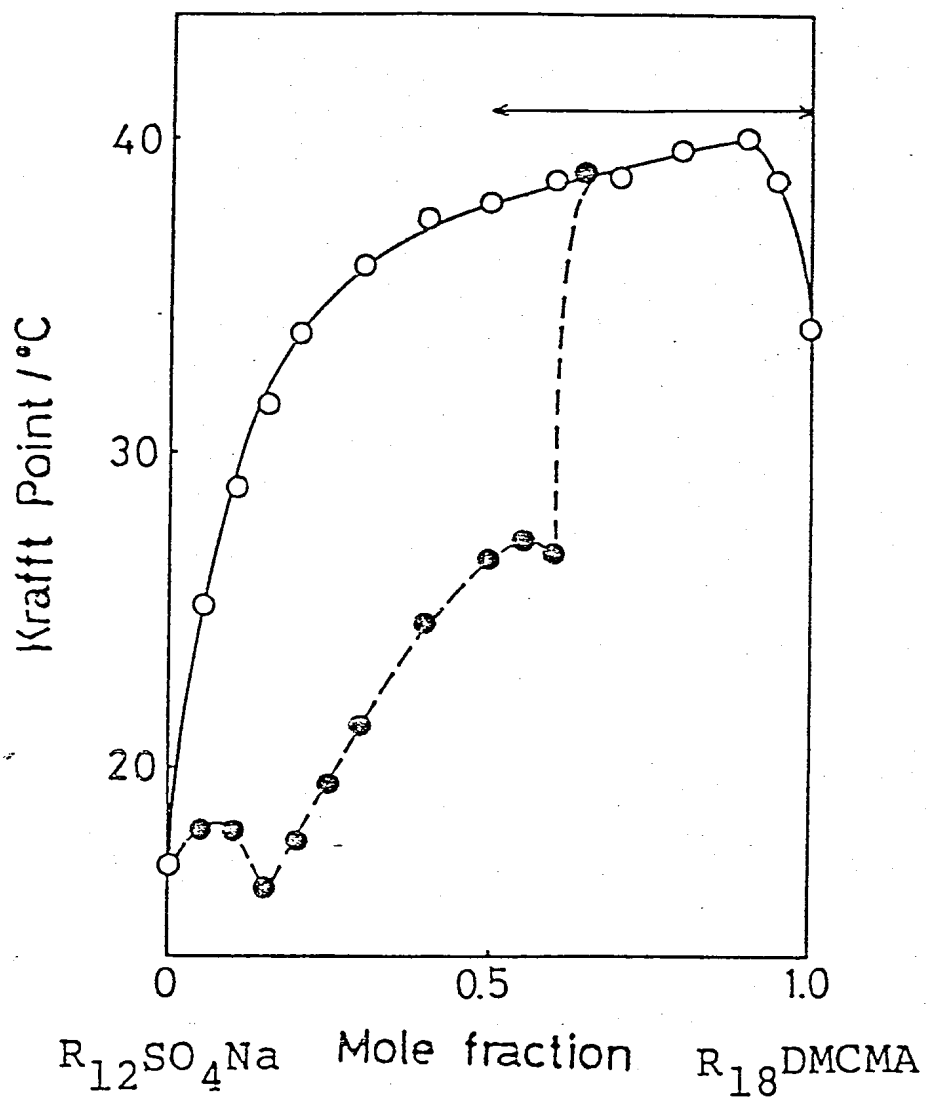


Figure 9. The Krafft point vs. composition curves of the $R_{12}SO_4Na/R_{18}DMCMA$ system. The upper (○) and the lower (●) curves show the Krafft point of the stable and the metastable solid phases, respectively. The arrows have the same meaning as those described in the legend of Figure 6.

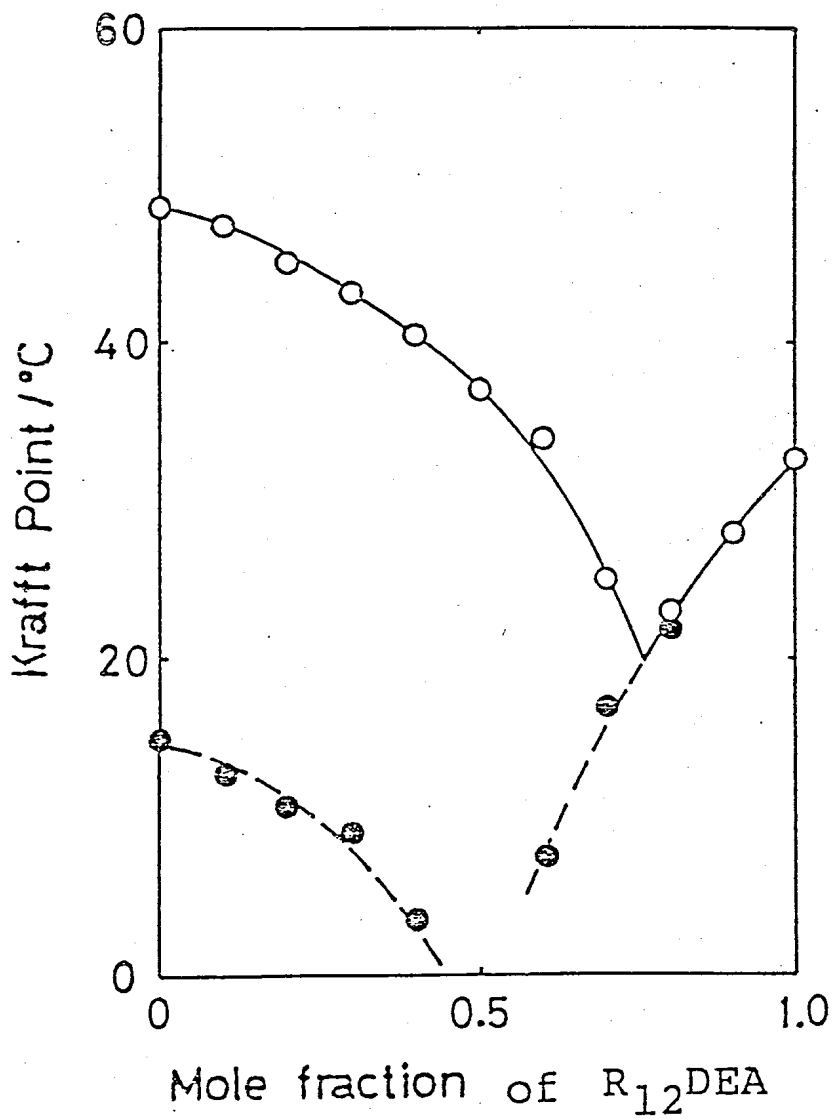


Figure 10. The Krafft point vs. composition curves of the $R_{12}SO_4Na$ (●) and $R_{14}SO_3Na/R_{12}DEA$ (○) systems.

$R_8\phi SO_3Na/R_{12}\phi SO_3Na$ system which has no minimum point, both components are mixed to form solid solutions.

Infrared Absorption Spectra.⁶⁶⁾ The results of the infrared absorption spectra of $R_{12}SO_4Na$, $R_{12}DMCMA$ and their addition compound are as follows; the absorption bands of $R_{12}SO_4Na$ at 1248 and 1217 cm^{-1} shift to 1257 and 1197 cm^{-1} respectively, and the absorption at 1083 cm^{-1} disappears in the spectrum of the addition compound. These results strongly suggest that the anionic sulfate group of $R_{12}SO_4Na$ plays an important role in the addition compound formation, since all the absorption bands mentioned above can be assigned to the S-O vibration of the $R_{12}SO_4Na$.

Viscoelasticity of the Solution.⁶⁶⁾ Most of the mixed solutions examined here between anionic and zwitterionic surfactants are found to be viscoelastic in a certain composition range. This composition range in each mixed solution indicated by the arrow (\longleftrightarrow) in Figures 6, 7, 8, and 9 is close to that of the Krafft-point maximum, i.e., the composition of each addition compound. The same viscoelastic behaviors have been observed also in the $R_{12}SO_4Na/R_{16}DMSPA$ system by Saul et al.⁶⁷⁾ The above result suggests that the addition compound or intermolecular complex might also be formed in micellar solution phases, since no

viscoelasticity can be observed in the solutions of each component.

Discussion

1. The Melting-Point Model for Krafft Temperature.

Qualitative Thermodynamic Descriptions for the Krafft-Point Change based on the Melting-Point Model. Once the melting-point model is accepted, the Krafft point change is predictable from thermodynamic theories. Let us consider thermodynamically the Krafft point vs. composition curves mentioned above, and give the new evidences for the melting-point model. The activity of a surfactant in liquid (micellar) phase is usually lowered by some additives. When an organic compound is solubilized into micelles or another surfactant is mixed, for instance, the mole fraction of the surfactant decreases in their mixed micelles. The activity coefficient of the surfactant will be depressed upon the addition of inorganic salts owing to the electrostatic interactions at the surface of the micelle. Such activity lowering in micellar phase causes the Krafft-point change, depending upon the activity of the surfactant in the solid phase.

1) When the activity in the solid phase is not altered by an additive, the Krafft point should be depressed just like the freezing-point depression of ordinary substances. The binary

surfactant mixtures in which both components do not mix with each other in the solid phase are the cases of the above, and should show an eutectic point in the Krafft point vs. composition curve.⁶⁸⁾

2) When two kinds of surfactant are completely miscible even in the solid phase to form a solid solution, the Krafft point must change monotonously with changing composition.⁶⁹⁾

3) If both components form an addition compound (or intermolecular compound) in the solid phase, a maximum may appear in Krafft point at a certain composition similarly to the melting point vs. composition curve in the mixtures of ordinary substances.⁷⁰⁻⁷³⁾ The quantitative arguments for each case will be made below.

Eutectic System. According to the thermodynamic theory for freezing-point depression⁶⁸⁾

$$\partial \ln a_i / \partial T = \Delta H^\circ_i / RT^2 \quad (i = 1 \text{ or } 2) \quad (1)$$

where a_i and ΔH°_i are the activity in the liquid (micellar) phase and the enthalpy of fusion of the pure i th component, respectively, and T is the melting temperature (Krafft point) expressed in absolute temperature. If one assumes that ΔH°_i is independent of temperature, eq 1 is integrated to give eq 2,

$$\ln a_i = -(\Delta H^\circ_i / R)(1/T - 1/T^\circ_i) \quad (2)$$

where T°_i is Krafft point of the pure i th component. Assuming ideal mixing of two types of anions (surface active ions) or cations (gegenions), we obtain eq 3,

$$\ln a_i = \nu_{i+} \ln X_{i+} + \nu_{i-} \ln X_{i-} \quad (3)$$

where ν_{i+} and ν_{i-} are the number of cations and anions, respectively, in the molecule of the i th component; and X_{i+} and X_{i-} are the fractions of cations and anions, respectively, of the i th component in the mixed micelle. The fractions X_{i+} and X_{i-} can be written as follows, since cations and anions do not mix with each other in the micellar phase:

$$X_{i+} = N_{i+} / (N_{1+} + N_{2+}) \quad (4)$$

$$X_{i-} = N_{i-} / (N_{1-} + N_{2-})$$

where N_{i+} and N_{i-} ($i = 1$ or 2) are the number of molecules of the i th component in the mixed micelle. Combining eq 2 and 3, we obtain eq 5.

$$\nu_{i+} \ln X_{i+} + \nu_{i-} \ln X_{i-} = -(\Delta H^{\circ}_i / R) (1/T - 1/T^{\circ}_i) \quad (5)$$

The first and second terms on the left side of eq 5 show the

contribution of the mixing of gegenions and surface-active ions, respectively, to the Krafft-point depression of pure *i*th component. Figure 11 shows the $-\ln X_{i+}$ vs. $1/T$ plots of the $R_{12}(\text{OE})\text{SO}_4\text{Na}/R_{12}(\text{OE})\text{SO}_4.1/2\text{Ca}$ mixtures. Good straight lines for both sodium and calcium salts are obtained. The values of ΔH°_i can be estimated from the slope of the straight lines. Unfortunately, evaluation of the ΔH°_i values for $R_8\phi\text{SO}_3\text{Na}$, $R_{12}\phi\text{SO}_3\text{Na}$ and $R_{15}(\text{OH})\text{SO}_3\text{Na}$ is impossible, since too few points are available to apply eq 5 (see Figures 1, 2, and 4). The calculated ΔH°_i values are listed in Table 4, together with those obtained from direct calorimetry (DSC). The ΔH°_i values obtained by both methods are in fair agreement, although only three sets of data are available to be compared.

System Displaying Complete Miscibility in the Solid Phase.

When two components are ideally mixed in both liquid and solid phases, the mole fraction of the second component in the liquid (micellar) phase (x_2^m) and that in the solid phase (x_2^s) can be written as follows:⁶⁹⁾

$$\begin{aligned} x_2^m &= (\exp(\lambda_1) - 1) / (\exp(\lambda_1) - \exp(-\lambda_2)) \\ x_2^s &= (\exp(\lambda_1) - 1) / (\exp(\lambda_1 + \lambda_2) - 1) \end{aligned} \quad (6)$$

where

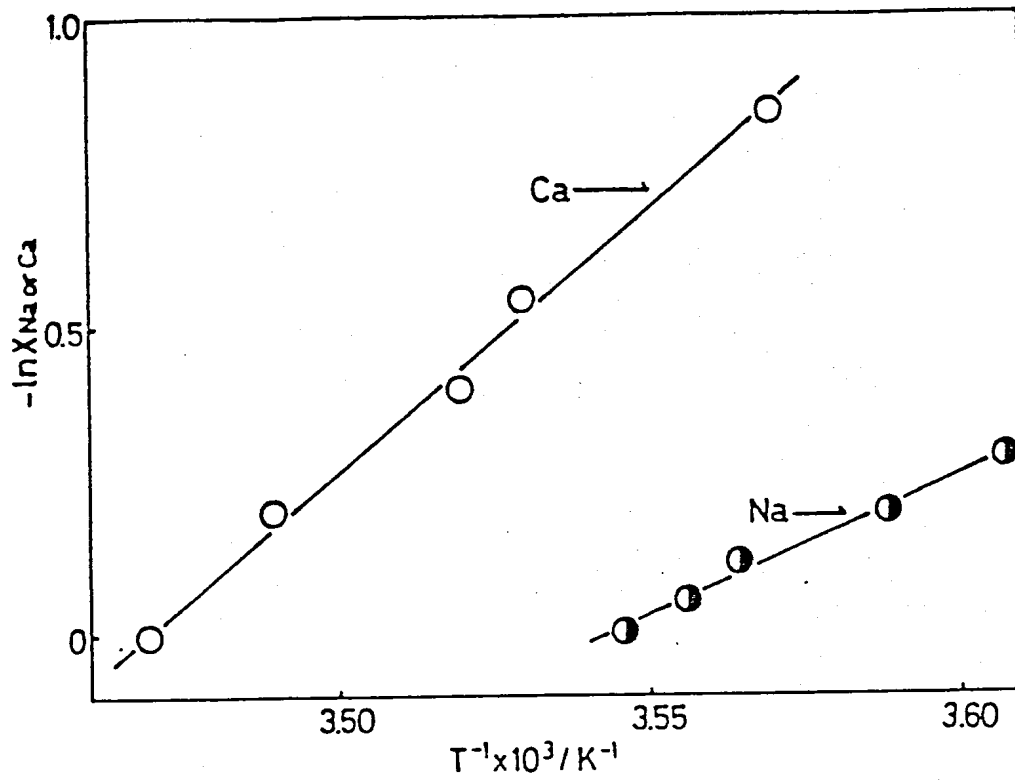


Figure 11. The plots of $-\ln X_{Na or Ca}$ against T^{-1} for the $R_{12}(OE)SO_4Na/R_{12}(OE)SO_4 \cdot 1/2Ca$ system.

Table 4: Transition enthalpies of pure surfactants at their Krafft points

surfactant	$H^{\circ a}/\text{KJ mol}^{-1}$			
	eq 5		DSC	
	Na salt	Ca salt	Na salt	Ca salt
$R_8 \phi \text{SO}_3$		193.1	10.4	
$R_{12} \phi \text{SO}_3$		253.3	26.3	
$R_{12}(\text{OE})\text{SO}_4$	39.3 ^b	82.8, ^c 69.0 ^b		89.4
$R_{15}(\text{OH})\text{SO}_3$		16.7 ^d	4.2	18.3
$R_{15}(\text{C}=\text{C})\text{SO}_3$	39.2 ^e	38.9, ^f 47.7 ^g	31.4	

a) One mole of sodium and calcium salts is based on the molecular structure of RSO_3Na and $(\text{RSO}_3)_2\text{Ca}$, respectively.

b) $R_{12}(\text{OE})\text{SO}_4(\text{Na}-1/2\text{Ca})$ system

c) $R_{12}(\text{OE})\text{SO}_4 \cdot 1/2\text{Ca}-R_8 \phi \text{SO}_3 \cdot 1/2\text{Ca}$

d) $R_{12}(\text{OE})\text{SO}_4\text{Na}-R_{15}(\text{OH})\text{SO}_3 \cdot 1/2\text{Ca}$

e) $R_{15}(\text{OH})\text{SO}_3\text{Na}-R_{15}(\text{C}=\text{C})\text{SO}_3\text{Na}$

f) $R_{15}(\text{C}=\text{C})\text{SO}_3(\text{Na}-1/2\text{Ca})$

g) $R_{15}(\text{OH})\text{SO}_3 \cdot 1/2\text{Ca}-R_{15}(\text{C}=\text{C})\text{SO}_3 \cdot 1/2\text{Ca}$

$$\lambda_1 = (\Delta H^\circ_1/R)(1/T - 1/T^\circ_1)$$

$$\lambda_2 = -(\Delta H^\circ_2/R)(1/T - 1/T^\circ_2)$$

Theoretical calculations are made for the $R_8 \phi SO_3Na/R_{12} \phi SO_3Na$ system using the ΔH°_1 and ΔH°_2 values listed in Table 4, and the results are shown in Figure 5 by dotted lines. The observed values are in poor agreement with the calculated curves, which may be due to the non-ideality of the solutions especially in the solid phase.

System Displaying Addition-Compound Formation. As mentioned previously, the Krafft point vs. composition curves have a maximum at a certain composition in the mixtures of anionic and zwitterionic surfactant. Similar maximum point can be seen in the melting point vs. composition curves of the ordinary substances when two components form an addition (intermolecular) compound in the solid phase.⁷⁰⁻⁷³⁾ The phenol/aniline system is a typical example of this case.⁷²⁾ The melting temperature vs. composition curve of this system is quite similar to those of $R_{12}SO_4Na/R_nDMSPA$ systems shown in Figure 6. The most convenient way to understand such curves is to imagine them to be made up of two curves of the simple eutectic type placed side by side.⁷²⁾ In the $R_{12}SO_4Na/R_nDMSPA$ systems, the curve of the left side is the $R_{12}SO_4Na$ /addition compound curve, and that of the right side is the R_nDMSPA /addition compound curve. It is clear from this interpretation for the Krafft point vs. composition

curves that the composition of the addition compound coincides with that of the Krafft-point maximum. The surfactant mixture having the composition of the addition compound should behave in every respect like a single "pure" component. In fact, the DSC curve at the composition of the Krafft-point maximum shows a single peak. The temperature at this peak is in good agreement with the Krafft point obtained from solution temperature. The Krafft temperature and the composition of the addition compound in several mixtures of anionic and zwitterionic surfactant are listed in Table 5.

Only one eutectic point has been observed in the R_{12} DMCMA and anionic surfactant systems as shown in Figures 7 and 8. It seems no eutectic point exists in the half side of the diagram (the side of R_{12} DMCMA/addition compound). If this is the case, the solid solution may form between R_{12} DMCMA and the addition compound, although this solid-solution formation cannot be confirmed because of too low Krafft point ($< 0^{\circ}\text{C}$) of R_{12} DMCMA. The $R_{12}\text{SO}_4\text{Na}/R_{18}$ DMCMA mixture gives somewhat complicated diagram. The Krafft point vs. composition curve of the metastable form (lower curve in Figure 9) has two maxima, indicating the existence of two kinds of addition compound having the composition of 9/1 and 1/1 in mole ratio. On the other hand, the stable solid shows one Krafft-point maximum, similarly to the other systems. The $R_{12}\text{SO}_4\text{Na}/$, and $R_{14}\text{SO}_3\text{Na}/R_{12}$ DEA systems are simple eutectic. (Fig. 10) This result may indicate that the electrostatic attractive force between

Table 5: Krafft temperature and the composition of the addition compound between anionic and zwitterionic surfactants

addition compound Anionics/Zwitterionics	composition in mole ratio	Krafft temp. /°C	
		solution temp.	DSC
$R_{12}SO_4Na/R_{12}DMSPA$	1/1	9.3	8
$R_{12}SO_4Na/R_{14}DMSPA$	1/1	21.3	21
$R_{12}SO_4Na/R_{16}DMSPA$	1/2	24.8	24
$R_{12}SO_4Na/R_{12}DMCMA$	2/3	37.6	37
$R_{12}SO_4Na/R_{18}DMCMA$	1/9 ^{a)}	40.1 ^{a)}	41 ^{a)}
$R_{12}SO_4Na/R_{12}DMAO$	1/3	25.8	
$R_{12}SO_4Na/R_{14}DMAO$	1/3	17.4	17
$R_{12}SO_4Na/R_{16}DMAO$	1/9	36.0	36
$R_{12}(OE)SO_4Na/R_{14}DMSPA$	1/1	6.9	
$R_{12}(OE)SO_4Na/R_{12}DMCMA$	2/3	7.0	
$R_{14}SO_3Na/R_{12}DMCMA$	1/2	36.2	
$R_{12}\phi SO_3Na/R_{12}DMCMA$	1/2	16.8	
$R_{15}(OH)SO_3Na/R_{12}DMCMA$	1/2	48.2	

a) Data for the stable solid phase (see text).

anionic and zwitterionic surfactant governs their addition-compound formation, because the zwitterionic agent has a cationic quarternary ammonium group and R_{12} DEA has not. The IR spectra of $R_{12}SO_4Na$, $R_{12}DMCMA$ and their addition compound may also support this assumption, since the absorption bands due to S-O vibrations of the anionic sulfate group of $R_{12}SO_4Na$ are strongly affected by the addition-compound formation.

Two cases should be taken into consideration in thermodynamic treatment of the Krafft point vs. composition curves. One is the case where the addition compound in the solid phase decomposes into individual component at its melting (Krafft) point. In the other case, the addition compound remains unchanged also in the micellar phase. For the first case, the Krafft point vs. composition curve can be written by eq. 7, assuming the ideal solutions in micellar phase,⁷⁰⁾

$$\ln X_1^{\nu_1} X_2^{\nu_2} = - \frac{\Delta H_m^\circ}{RT_K} + \text{const.} \quad (7)$$

where the symbols used in eq. 7 are as follows:

- x_1 and x_2 ; mole fraction of component 1 and 2
 respectively in liquid (micellar) phase.
- ν_1 and ν_2 ; number of molecules of component 1 and 2
 respectively in one addition compound.
- ΔH_m° ; enthalpy of fusion of "pure" addition
 compound.
- R ; gas constant
- T_K ; Krafft point expressed by absolute
 temperature.

If the addition compound does not decompose when it melts, the equation for simple eutectic system can be applied to each half side of the diagram shown in Figures 6, 7, 8, and 9. Then, we obtain

$$\ln X_c = -\frac{\Delta H_m^\circ}{R} \left(\frac{1}{T_K} - \frac{1}{T_K^\circ} \right) \quad (8)$$

where X_c is the mole fraction of the addition compound in micellar phase, and T_K° the Krafft point of "pure" addition compound. The fraction X_c can be readily calculated, and expressed in terms of x_1 , x_2 , and ν_1 and ν_2 as follows.

$$x_c = \frac{x_2}{x_2(1 - v_1 - v_2) + v_2} \quad \text{for } x_1 > \frac{v_1}{v_1 + v_2} \quad (9)$$

or

$$x_c = \frac{x_1}{x_1(1 - v_1 - v_2) + v_1} \quad \text{for } x_1 < \frac{v_1}{v_1 + v_2} \quad (10)$$

Figure 12 shows both plots of eq. (7) and (8) for the $R_{12}SO_4Na/R_{14}DMAO$ system. As is clear from Figure 12, the plot of eq. (8) gives a straight line, but that of eq. (7) does not. For some other systems, however, both plots of eq. (7) and (8) give the straight lines. In such cases, the ΔH_m° values are calculated from the slope of the straight lines, and compared with those from direct calorimetry (DSC). The calculated ΔH_m° values for several systems are listed in Table 6, together with those from DSC. One can see from the table that the ΔH_m° values from eq. (8) show better agreement with those from DSC. These results may suggest that the addition compounds are present, not only in solid phases but also in micellar solution phases. The viscoelasticity of the solution in the composition range close to that of the addition compound also supports this conclusion, as mentioned previously. Furthermore, the interaction energy between $R_{12}SO_4Na$ and $R_{12}DMSPA$ ($-7.8RT$) in aqueous solutions⁷⁴⁾ is sufficiently large for addition-compound formation, since the complex formation in the $R_{12}\phi SO_3Na/R_{12}DMAO$

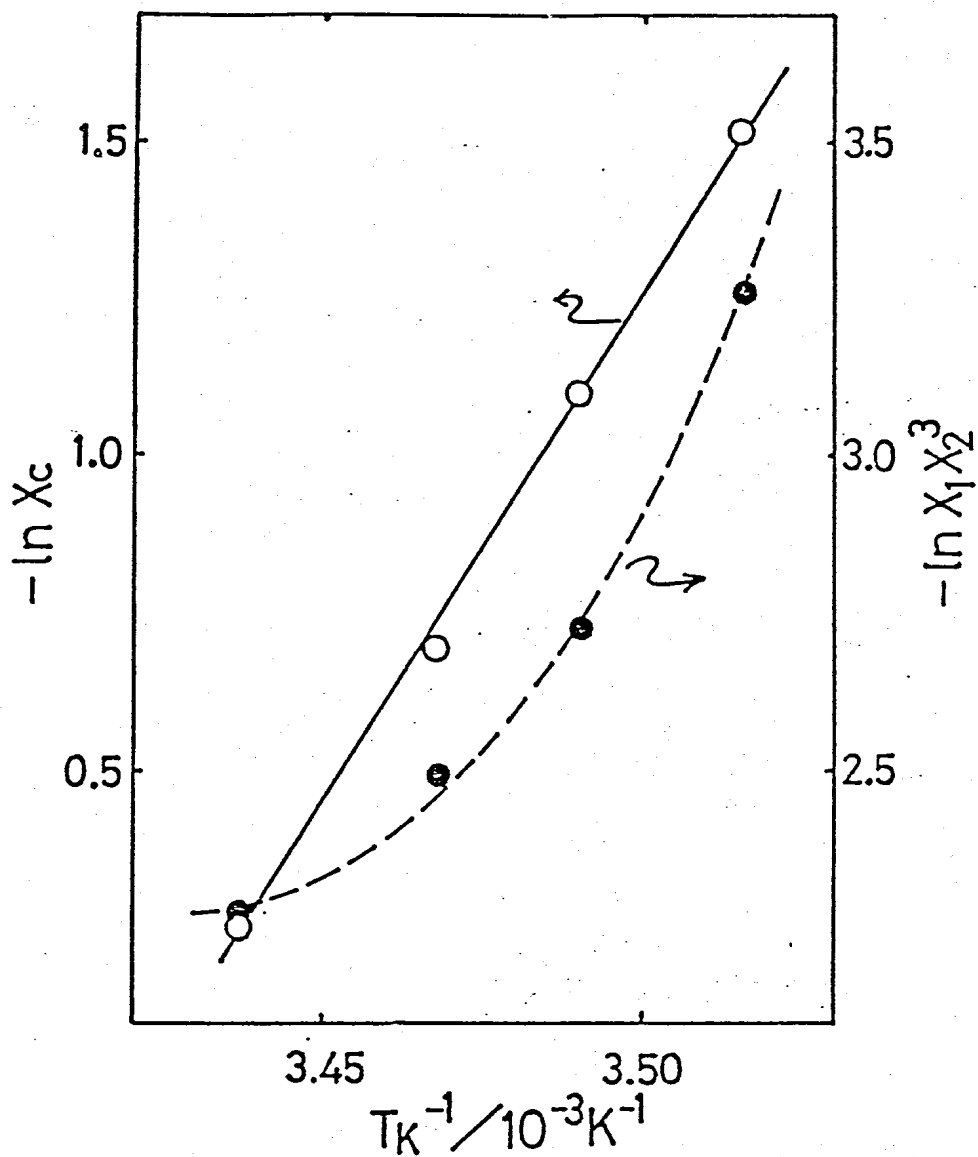


Figure 12. The plots of $-\ln X_1^{\nu_1} X_2^{\nu_2}$ (●) or $-\ln X_c$ (○) against T_K^{-1} for the $R_{12}SO_4Na/R_{14}DMAO$ system.

Table 6: Transition enthalpies of addition compounds from Eq.(7), Eq.(8) and direct calorimetry (DSC).

addition compound	$\Delta H_m^\circ / \text{KJ.mol}^{-1}$		
	DSC	Eq. (7)	Eq. (8)
$R_{12}SO_4Na/R_{12}DMSPA$	34	24	39
$R_{12}SO_4Na/R_{14}DMSPA$	38	12	31
$R_{12}SO_4Na/R_{16}DMSPA$	24	11	16
$R_{12}SO_4Na/R_{12}DMCMA$	14	11	14
$R_{12}SO_4Na/R_{14}DMAO$	26		34

mixture is known⁷⁵⁾ in spite of smaller interaction energy (-3.5RT) than that of the above mixture.⁷⁴⁾

Addition-compound (or complex) formation in the solution phases has already been reported by several authors for $R_{12}\text{DMAO}/$, and 3-(dodecylammonio)-propionate/anionic surfactant mixtures.⁷⁵⁻⁷⁸⁾ According to their results, the composition of the complex is 1/1 in mole ratio for all the above systems. If the mole ratios of the addition compounds in solution phases are 1/1 also in our systems, the thermodynamic treatments described above are not exactly correct, since equation(8) is derived assuming the same composition of the compound in the solution phases as that in the solid phases. Possible partial decomposition of the solid addition-compound at the Krafft point may be also unfavorable for the exact application of eq.(8). These are possible reasons why the ΔH_m° values calculated from eq.(8) do not agree so well with those values from DSC.

2. Applicability of Anionic Surfactant in Hard Water.

As is clear from Figure 1, the Krafft points of $R_8\phi\text{SO}_3\text{Na}$ and $R_{12}\phi\text{SO}_3\text{Na}$ are elevated abruptly by the presence of small amounts of the calcium salts. This result indicates that the alkylbenzenesulfonates are not applicable in hard water without any sequestering agents. Figure 13 shows the effect of added sodium

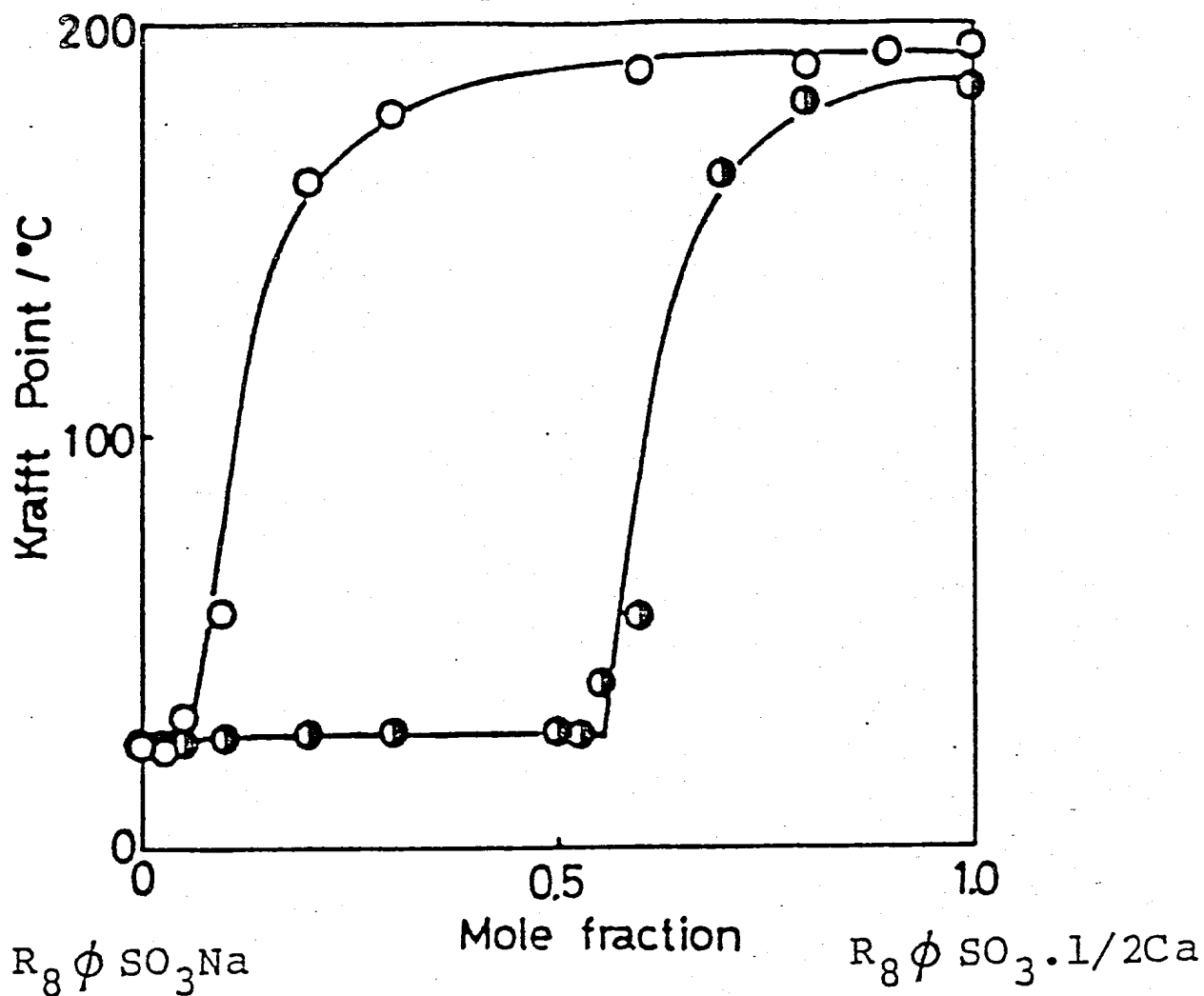


Figure 13. The Krafft point vs. composition curves of the $R_8\phi SO_3Na/R_8\phi SO_3 \cdot 1/2Ca$ system in the absence (\circ) and presence (\bullet) of sodium nitrilotriacetate. The concentration of NTA was kept constant at 17mM (half of the total amounts of surfactant).

nitrilotriacetate (NTA) on the Krafft points of the $R_8\phi SO_3Na/R_8\phi SO_3 \cdot 1/2Ca$ mixtures. The Krafft points of the above mixtures are maintained constant at the same level as that of $R_8\phi SO_3Na$, unless calcium salt concentration exceeds the chelating capacity of NTA. Krafft-point change of the $R_{15}(OH)SO_3Na$ and $R_{15}(C=C)SO_3Na$ upon the addition of the corresponding calcium salts is similar to that of the alkylbenzenesulfonates, although the Krafft points of the calcium salts are much lower than those of $R_n\phi SO_3 \cdot 1/2Ca$ (Figure 2). It is clear from the figure that a sequestering agent is useful (or necessary) for practical uses of α -olefin sulfonates in hard water. One can easily realize from Figure 3 and Table 3 that the alkylpoly(oxyalkylene) sulfates are the best one among the surfactants tested. They may be applicable in hard water without any sequestering agents. Figure 14 shows the effect of blended $R_{12}(OE)_nSO_4 \cdot 1/2Ca$ ($n = 1, 3$) on the Krafft point of $R_8\phi SO_3 \cdot 1/2Ca$. Dodecylmono- or -tris(oxyethylene) sulfate depresses the Krafft point of $R_8\phi SO_3 \cdot 1/2Ca$ considerably. Alkylpoly(oxyethylene) sulfates may help the applicability of alkylbenzenesulfonates in hard water. The applicability of alkylpoly(oxypropylene) sulfates in hard water seems to be better than the sulfates with poly(oxyethylene) group from the Krafft points of sodium salts (Table 3). It is indeed confirmed that the tolerance of the surfactants for calcium ions (hard water) is excellent.⁶²⁾

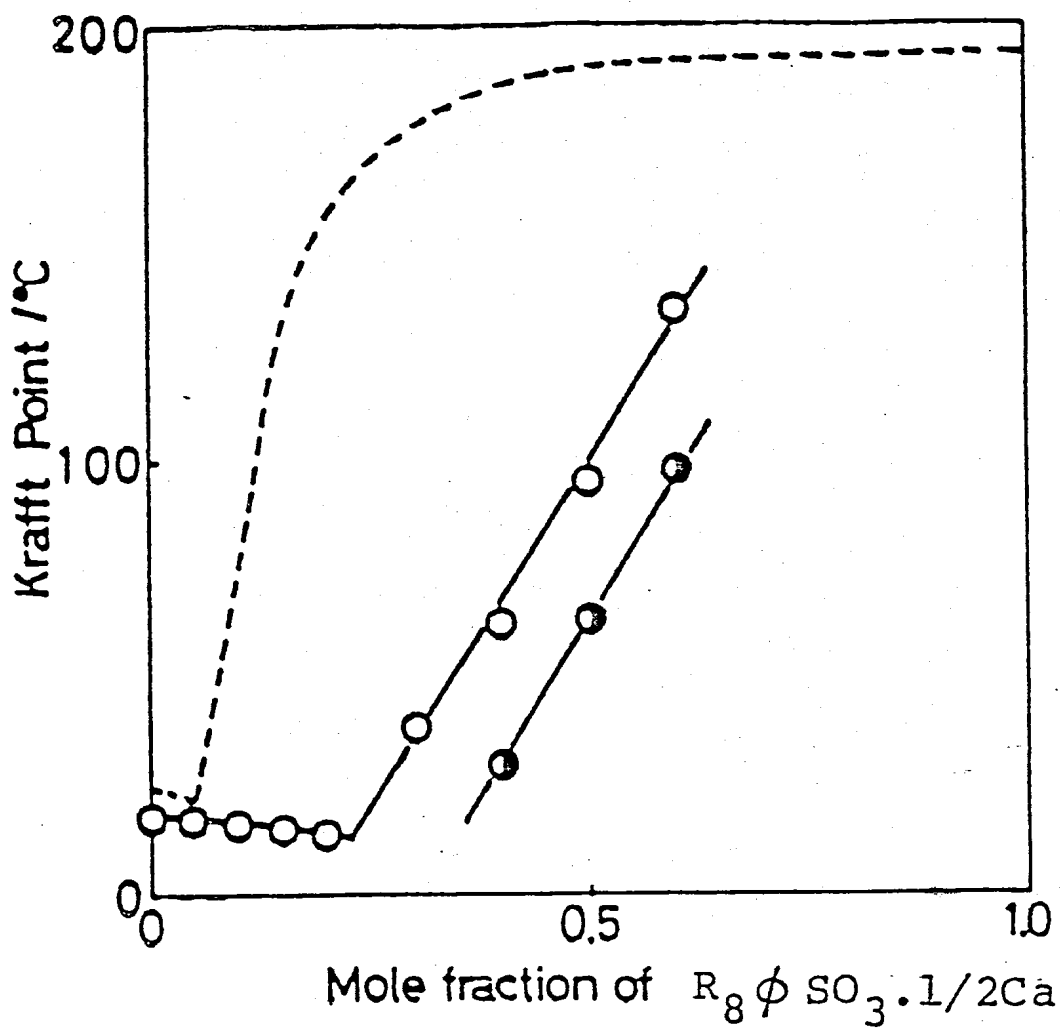


Figure 14. The Krafft point vs. composition curves of the $R_{12}(OE)SO_4 \cdot 1/2Ca/R_8\phi SO_3 \cdot 1/2Ca$ (○), $R_{12}(OE)_3SO_4 \cdot 1/2Ca/R_8\phi SO_3 \cdot 1/2Ca$ (●) and $R_8\phi SO_3Na/R_8\phi SO_3 \cdot 1/2Ca$ (dotted line) systems.

Part II

Krafft-Point Depression of Some Zwitterionic Surfactants by Inorganic Salts

Introduction

The Krafft point of ionic surfactants is well-known to be elevated upon the addition of inorganic salts.^{14,42,79,80} This same salting-out phenomenon has also been reported even in the nonionic surfactant solutions, although the extent of the Krafft-point elevation is small.⁸¹ Such salting-out of the surfactant frequently causes the phase separation (solid-precipitation) troubles in liquid detergents and/or shampoos. Although added salts lower the cmc, and enhance the surface activity of a surfactant, we cannot formulate the inorganic salts so much because of the above reason.

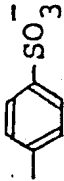
The Krafft point of some zwitterionic surfactants, however, is interestingly found to be depressed upon the addition of inorganic salts.^{82,83} This newly-found salting-in phenomenon of zwitterionic surfactants have been treated thermodynamically, and presented as an another evidence for the melting-point model of Krafft point.

Experimental Section

Materials. Surfactant samples used in Part II are listed in Table 7. The samples which are already described in Part I are omitted from the table. R_{18} DMCPA was prepared as follows; N,N-dimethyloctadecylamine was reacted with methyl (γ -iodo)butyrate, and then the reaction product was passed through an anion exchange resin.⁸⁴⁾ The final product was recrystallized from acetone/ethanol mixture. N,N-Dimethyl-N-benzyltetradecylammonium chloride was allowed to react with fuming sulfuric acid in 95% H_2SO_4 to obtain $R_{14}DM\phi SA$. The reaction product was purified by the repeated recrystallization from ethanol. R_{12} CEA was a kind gift from Mr. T. Okumura of Tokyo Research Laboratories, Kao Soap Company, and the same used in his previous work.⁸⁵⁾ R_{18} TMAC was purchased from Tokyo Kasei Ltd., and used without further purification. Inorganic salts obtained from Wako Pure Chemicals Co. were of guaranteed reagent grade and used without purification. Deionized and distilled water was used to prepare the sample solutions.

Krafft-Point Determinations. The procedures of Krafft-point measurements were described already in Part I. The Krafft points of R_{12} CEA were measured at its isoelectric point ($pH = 6.6 \pm 0.1$ ⁸⁶⁾). The pH of the solutions was adjusted with NaOH or HCl.

Table 7: Surfactant samples used in Part II and their abbreviations.

Name of surfactant	Molecular structure	Abbreviation
N,N-Dimethyl-N-(3-carboxypropyl) octadecylammonium inner salt	$n\text{-C}_{18}\text{H}_{37}\overset{+}{\text{N}}(\text{CH}_3)_2\text{CH}_2\text{CH}_2\text{CH}_2\text{COO}^-$	R ₁₈ DMCPA
N,N-Dimethyl-N-(4-sulfobenzyl) tetradecylammonium inner salt	$n\text{-C}_{14}\text{H}_{29}\overset{+}{\text{N}}(\text{CH}_3)_2\text{CH}_2\text{-}$ 	R ₁₄ DMφSA
N-(2-Carboxyethyl)dodecylamine	$n\text{-C}_{12}\text{H}_{25}\overset{+}{\text{N}}\text{H}_2\text{CH}_2\text{CH}_2\text{COO}^-$	R ₁₂ CEA
N,N,N-Trimethyloctadecylammonium chloride	$n\text{-C}_{18}\text{H}_{37}\text{N}(\text{CH}_3)_3\text{Cl}$	R ₁₈ TMAC

Cmc Measurements. The cmc values of R_{12} CEA and $R_{12}SO_4Na$ in the absence and presence of NaCl were determined by surface tension measurements which were carried out by the drop volume method. The pH of the R_{12} CEA solutions was adjusted at 6.6 ± 0.1 with NaOH or HCl prior to surface tension measurements.

Differential Scanning Calorimetry. Differential scanning calorimetry was performed in the same manner as that described in Part I.

^{13}C -NMR Spectra. ^{13}C -NMR measurements were carried out with a JEOL-PFT-100 pulse-Fourier-transform NMR spectrometer (25MHz) at room temperature. The concentration of surfactant was kept constant at 10 wt%. Deuterium oxide was used as a solvent to obtain the NMR lock signal.

Results

In Figure 15, the values of $(T_K - T_K^0)/T_K (= \Delta T_K/T_K)$ are plotted against $C_S^{1/2}$ for various types of surfactant, where T_K and T_K^0 are the Krafft points in the presence and absence of NaCl, respectively, and C_S is the molar concentration of NaCl.

The Krafft points of cationic ($R_{18}\text{TMAC}$) and anionic ($R_{12}\text{SO}_4\text{Na}$) surfactant are remarkably elevated on addition of NaCl. Even nonionic surfactant (octadecyl polyoxyethylene ether with 10 oxyethylene units) shows a small increase of Krafft point with added salt.⁸¹⁾ On the other hand, the Krafft point of the zwitterionic surfactants examined here decreases with increasing concentration of NaCl. Note in this figure that the $\Delta T_K/T_K$ values are linearly related to $C_S^{1/2}$ for the zwitterionic surfactants, the $\Delta T_K/T_K$ vs. $C_S^{1/2}$ plot for $R_{18}\text{DMSPA}$ breaks at about 0.1 M NaCl, and the slope of the straight line of $R_{18}\text{DMSPA}$ above 0.1 M NaCl is very similar to that of $R_{16}\text{DMSPA}$. The Krafft point vs. $C_S^{1/2}$ curves for the other zwitterionic surfactants are shown in Figures 16 and 17. One can see from these two figures that all zwitterionic surfactants are not necessarily salted-in. Figures 18-20 show the effect of the nature of added salt on the Krafft point change of R_{16}^- , $R_{18}\text{DMSPA}$ (Fig. 18), $R_{18}\text{DMCMA}$ (Fig. 19), and $R_{18}\text{DMCPA}$ (Fig. 20). The governing factor to distinguish between the salting-in and salting-out type of the zwitterionic surfactant seems to be the molecular structure of the agent, since the kind of added salt does not alter the tendency of the Krafft-point change.

The temperature dependence of $R_{18}\text{DMSPA}$ solubility is shown in Figure 21. The log (solubility) vs. $1/T$ plots are linear below the Krafft temperature, which indicates that the enthalpy change of solution is constant (99.8 kJ/mol from the slope) in the temperature

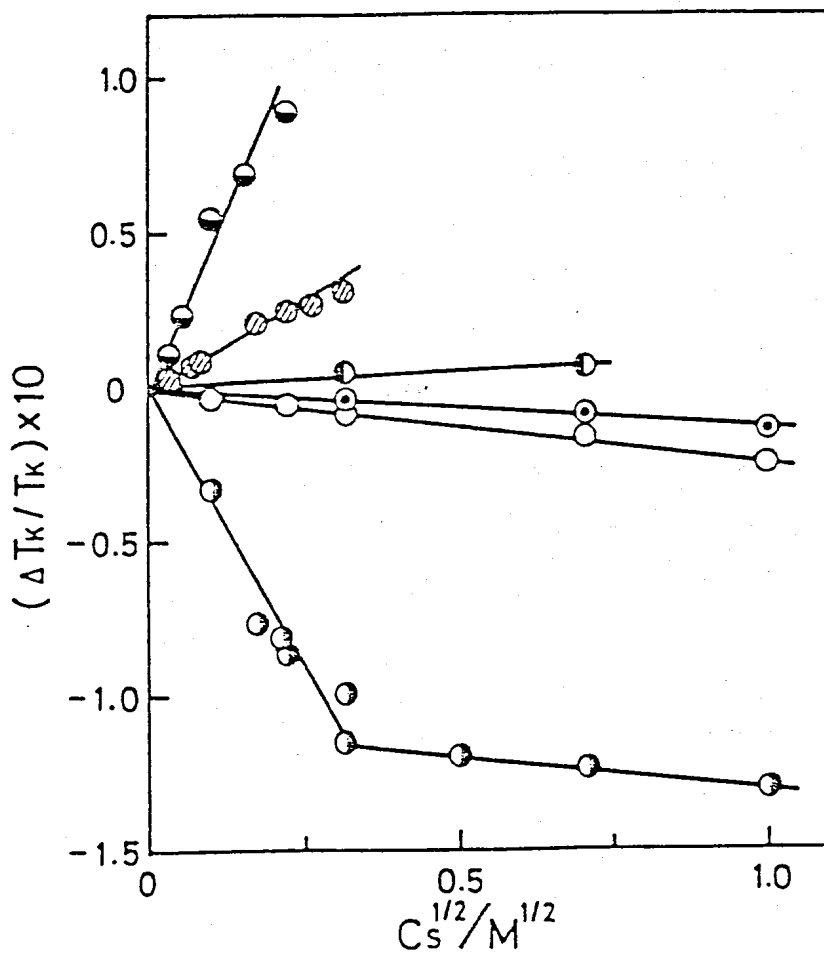


Figure 15. The $\Delta T_K/T_K$ vs. $C_s^{1/2}$ plots for various surfactants in aqueous NaCl solutions: 10mM R_{18} TMAC (\ominus), 10mM $R_{12}SO_4Na$ (\otimes), 1% octadecylpolyoxyethylene ether (\oplus), 2mM R_{16} DMSPA (\odot), R_{12} CEA (\circ), and R_{18} DMSPA ($\opl�$). The data for octadecylpolyoxyethylene ether were taken from Ref.81.

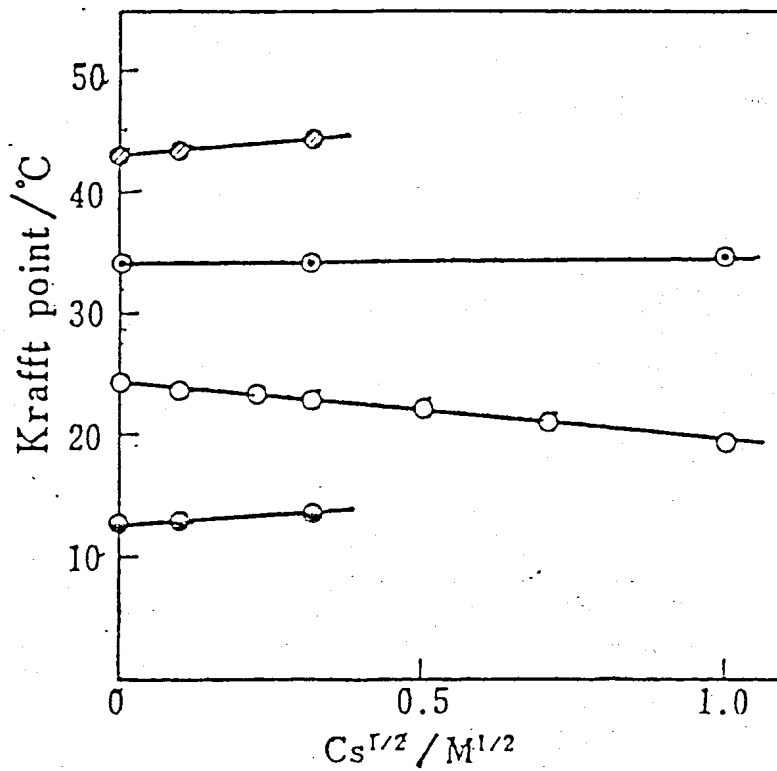


Figure 16. Krafft points of $R_{16}DMCMA$ ($\text{\textcircled{h}}$), $R_{18}DMCMA$ ($\text{\textcircled{\bullet}}$), $R_{18}DMCPA$ ($\text{\textcircled{\circ}}$), and $R_{18}DMAO$ ($\text{\textcircled{h}}$) in aqueous NaCl solutions.

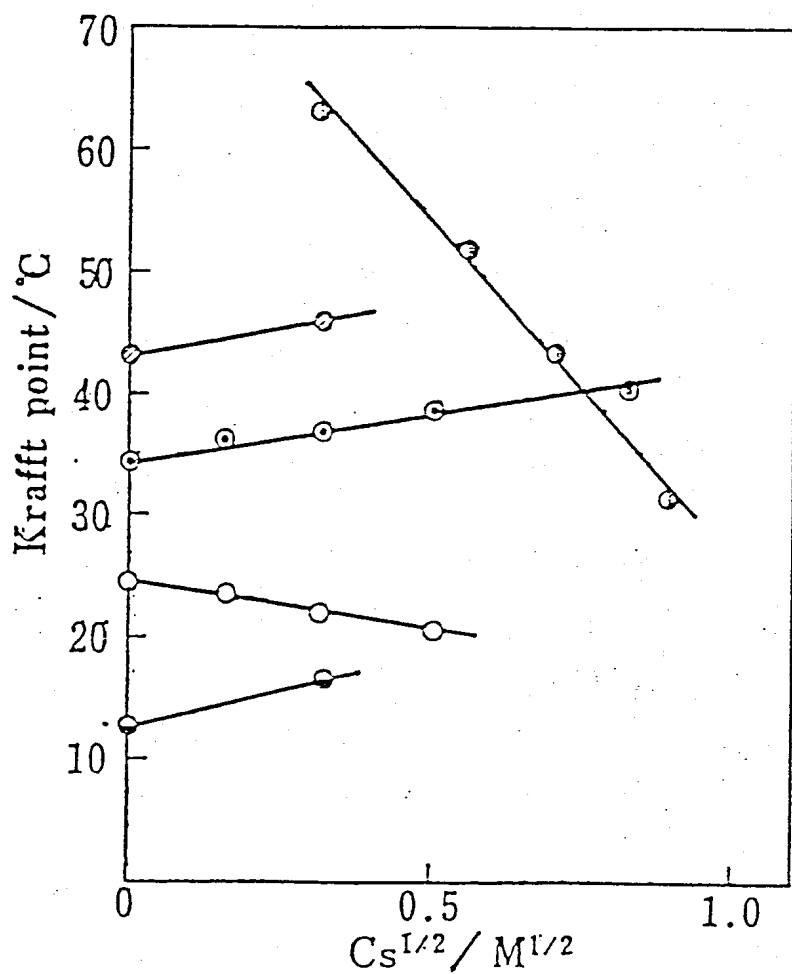


Figure 17. Kraft points of $R_{16}DMCMA$ (\ominus), $R_{18}DMCMA$ (\odot), $R_{18}DMCPA$ (\circ), $R_{18}DMAO$ (\otimes), and $R_{14}DM\phi SA$ (\oplus) in aqueous NaSCN solutions.

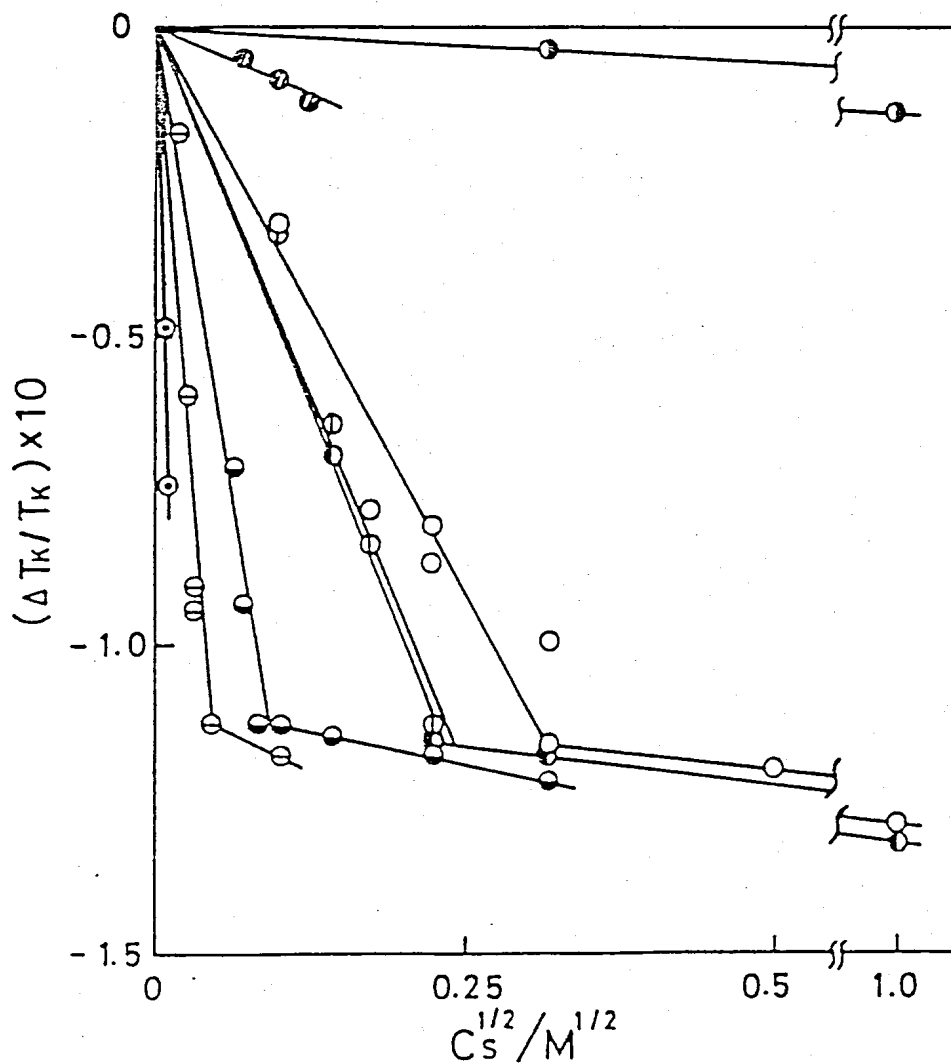


Figure 18. The $\Delta T_K/T_K$ vs. $C_s^{1/2}$ plots for R_{16}^- and R_{18} DMSPA in the presence of various added salt: R_{16} DMSPA-NaCl (\odot), -NaSCN (\otimes); R_{18} DMSPA-NaCl (\circ), NH_4Cl (\ominus), -KCl (\oplus), - $NaNO_3$ ($\omin�$), -NaI ($\omin�$), and -NaSCN (\odot).

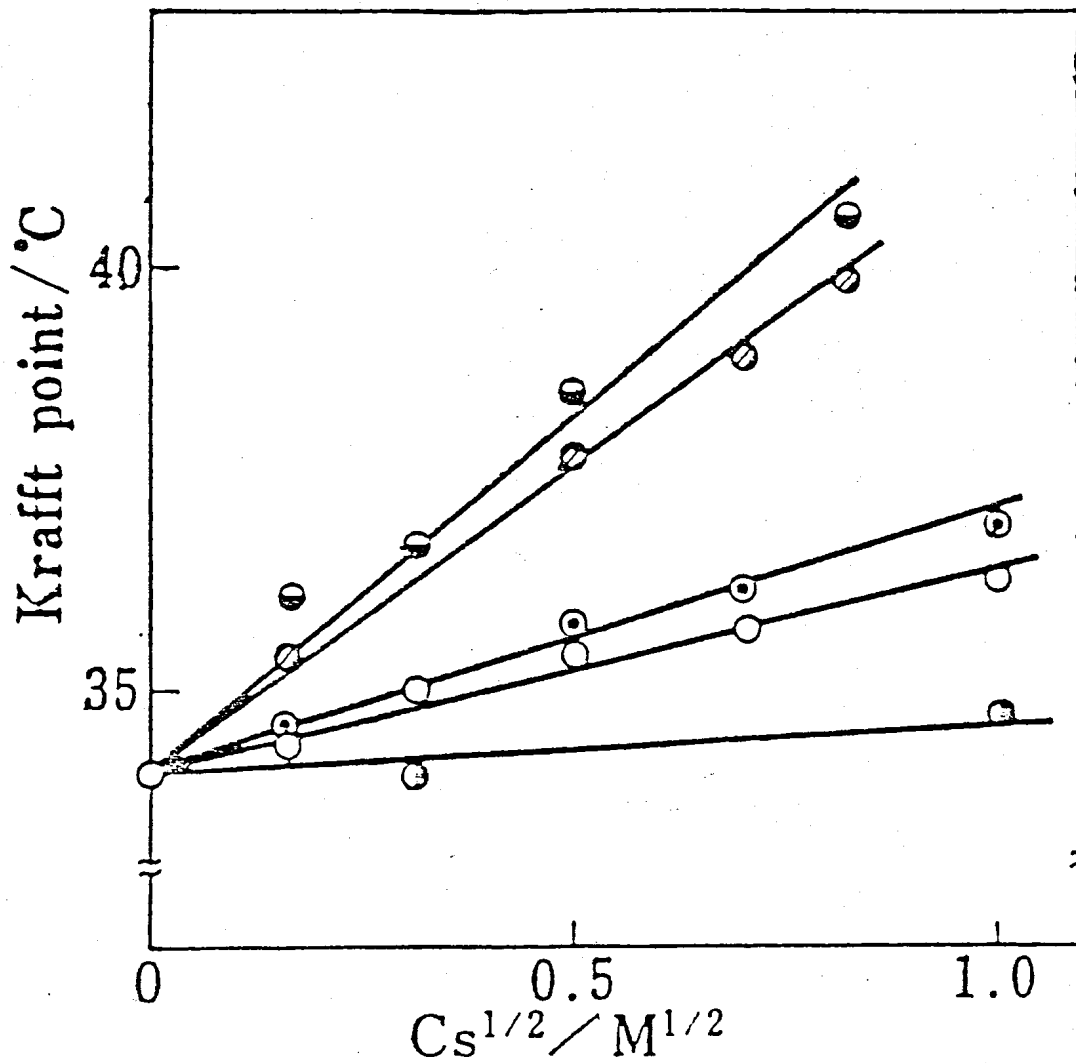


Figure 19. Krafft points of R_{18} DMCMA in aqueous salt solutions. Added salts are NaCl (\odot), NaBr (\circ), $NaNO_3$ (\odot), NaI ($\textcircled{//}$), and NaSCN (\ominus).

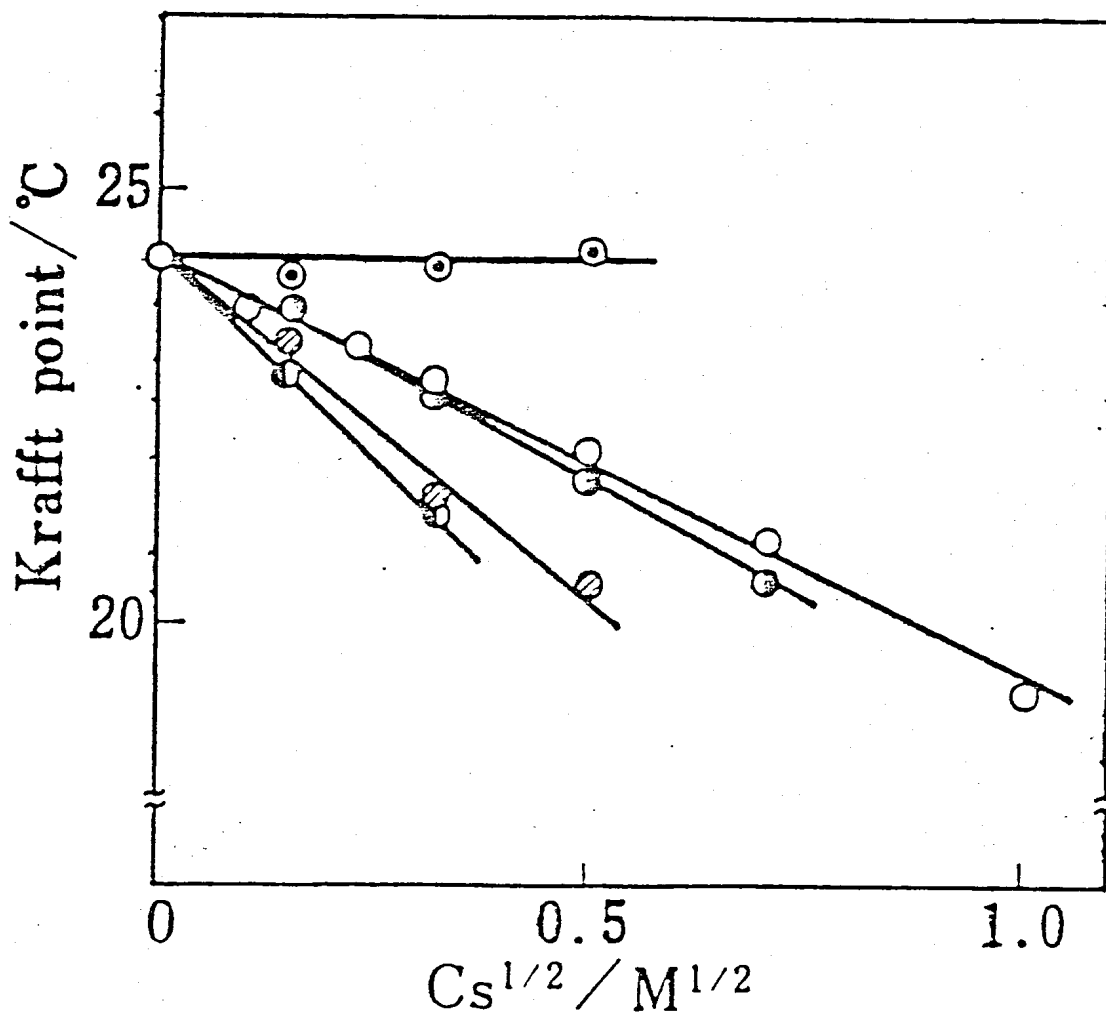


Figure 20. Krafft points of R_{18} DMCPA in aqueous salt solutions.

Added salts are $NaNO_3$ (●), $NaSCN$ (▨), $LiCl$ (◐),
 $NaCl$ (○), and Na_2SO_4 (◉).

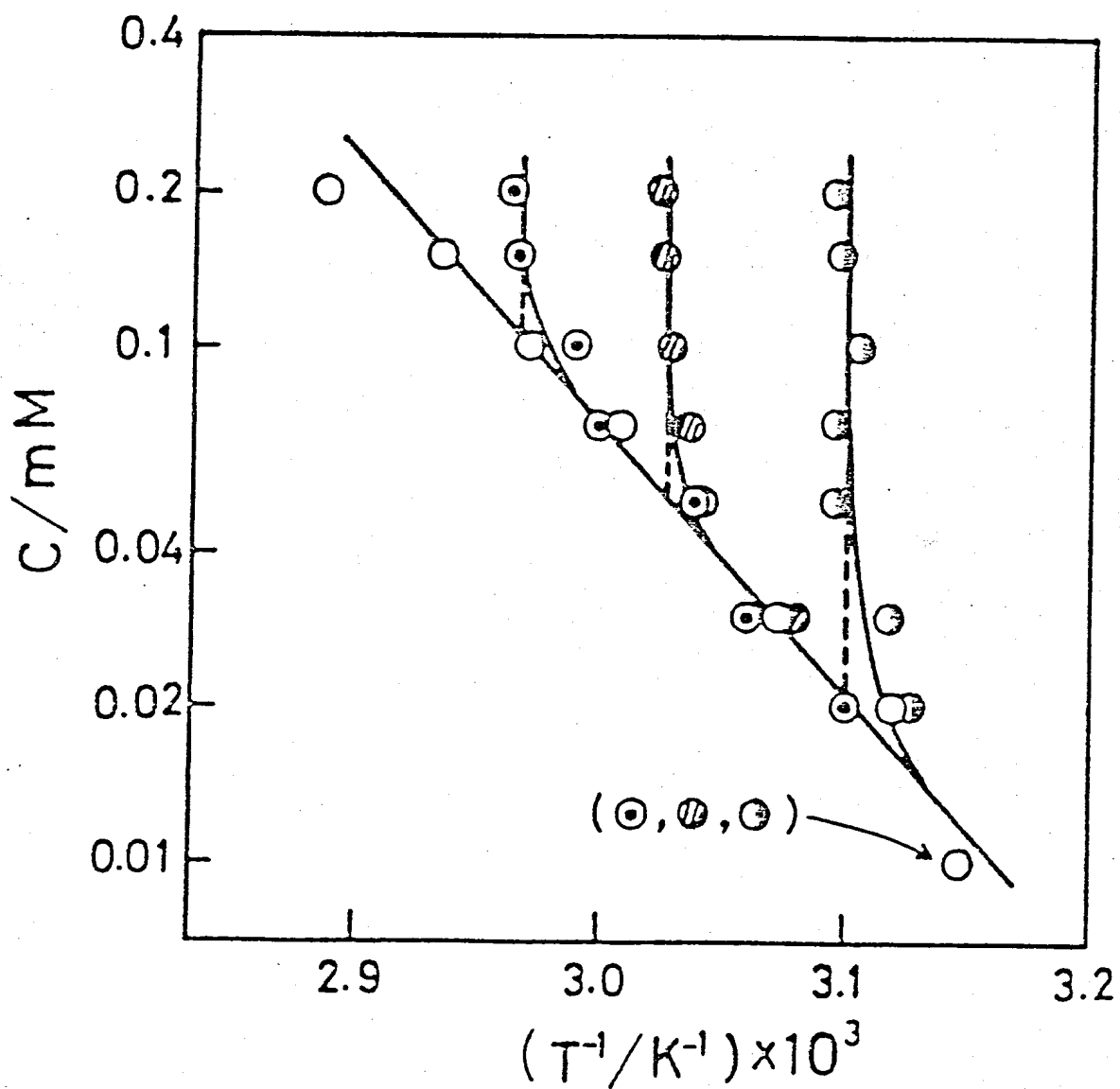


Figure 21. The log (solubility of R₁₈DMSPA) plotted against T⁻¹ in pure water (○), 0.05mM NaSCN (⊙), 0.06mM NaSCN (⊘), and 0.10mM NaSCN (⊗).

range examined here. It can be seen further that the activity coefficient of the surfactant monomer does not change on addition of salt (NaSCN), since all data below the Krafft point fall on the same straight line.

The cmc values of R_{12} CEA and $R_{12}SO_4Na$ in aqueous NaCl solutions are given in Table 8.

The transition temperatures and enthalpies of R_{16}^- and R_{18} DMSPA obtained by differential scanning calorimetry are listed in Table 9. The transition temperatures of R_{16} DMSPA as well as R_{18} DMSPA at NaCl concentrations above the break point (≈ 0.1 M NaCl) are in good agreement with the Krafft points determined photometrically. However, a transition at temperatures below the Krafft point was observed for R_{18} DMSPA in the solutions of low NaCl concentration. Microscopic observations under crossed polarizers were made below and above the transition temperature ($37.2^\circ C$). Figure 22 presents photographs of R_{18} DMSPA dispersions in the absence of NaCl. Fine crystalline precipitates can be observed below $37.2^\circ C$ as expected. Above the transition temperature, however, the typical texture of liquid crystalline droplets⁸⁷⁻⁹⁰ is found as shown in Figure 22. The Krafft point observed photometrically can be attributed to the transformation of liquid crystalline droplets into transparent micelles.

The ^{13}C -NMR chemical shifts of some zwitterionic surfactants in pure water and aqueous salt solutions are given in Table 10.

Table 8: The cmc values of R_{12} CEA and $R_{12}SO_4Na$ in aqueous NaCl solutions

NaCl concn/ M	cmc ^a /mM	
	R_{12} CEA	$R_{12}SO_4Na$
0.00	1.65	8.20
0.001		8.10
0.005		6.80
0.007		6.20
0.01	1.43	
0.03		3.40
0.05	1.35	2.44
0.07		2.01
0.10	1.18	1.71
0.50	0.87	
1.00	0.66	

a) Measured at 40°C for R_{12} CEA and at 25°C for $R_{12}SO_4Na$

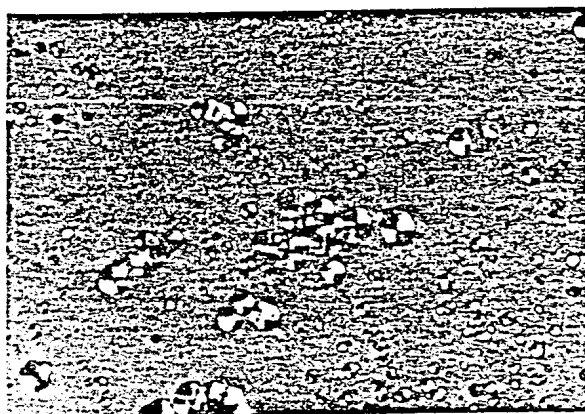
Table 9: Phase transition temperatures and enthalpies of R_{16} DMSPA and R_{18} DMSPA in aqueous NaCl solutions^a

NaCl concn/M	R_{16} DMSPA		R_{18} DMSPA	
	temp./°C	enthalpy/KJ·mol ⁻¹	temp./°C	enthalpy/KJ·mol ⁻¹
0	28.0	67.6	37.2 ^b	76.0 ^b
0.01			37.5 ^b	70.1 ^b
0.05			36.8 ^b	71.8 ^b
0.10	26.8	68.0	36.8	70.8
0.50			34.6	68.0
1.00			33.2	64.9

a) The concentration of R_{16} DMSPA or R_{18} DMSPA was kept constant at 20 mM. b) Transition temperatures or enthalpies of hydrated crystalline-liquid crystalline phase transition (see text).



A



B

Figure 22. Microscopic photographs (X 100) under crossed polarizers of R_{18} DMSPA dispersions in pure water, below (A) and above (B) the transition temperature (37.2°C).

No appreciable change of chemical shift was observed in other signals than those shown in Table 10 upon the addition of the inorganic salts. The signals due to N-methyl and N-methylene carbons of R₁₆DMSPA (salted-in type) are shifted much more greatly than those of R₁₆DMCMA by added salts.

Discussion

As mentioned previously, Krafft-point depression of zwitterionic surfactants by inorganic salts is very interesting and unusual phenomenon, since any other types of surfactants do not exhibit such behavior at all. Let us consider first why only zwitterionic agent can be salted-in. According to the thermodynamic theory for freezing-point depression⁶⁸⁾

$$\partial \ln a / \partial T_K = \Delta H_m^\circ / RT_K^2 \quad (11)$$

where a is the activity of the surfactant in the liquid (micellar) phase, ΔH_m° the enthalpy of fusion, and T_K the melting temperature (Krafft point) expressed in absolute temperature. Integrating eq. 11 under the condition of temperature independence of ΔH_m° , we obtain

Table 10: ^{13}C -NMR Chemical shifts of zwitterionic surfactants in pure water and aqueous salt solutions.

Surfactant	Medium	Chemical shift ^{a)}	
		N-methyl	N-methylene ^{b)}
$\text{R}_{16}\text{DMSPA}$	pure water	929.2	1210.9 1256.8
	0.1M NaCl	924.8	1218.3 1266.8
	0.1M NaSCN	915.5	1225.0 1280.8
$\text{R}_{16}\text{DMCMA}$	Pure water	935.4	1257.3
	0.14M NaSCN	933.4	1264.9

- a) Herz from the signal due to terminal methyl group of the hydrocarbon chain.
- b) Two N-methylene signals were observed separately for $\text{R}_{16}\text{DMSPA}$, and listed together, since we could not assign them. Only one N-methylene signal was observed for $\text{R}_{16}\text{DMCMA}$, although the reason for this observation is not clear.

$$-\ln a = (\Delta H_m^\circ / RT_K) + K \quad (12)$$

where K is an integration constant. From eq.12, we can derive the next equation.

$$\ln \frac{a}{a^0} = \frac{\Delta H_m^\circ}{RT_K^0} \cdot \frac{\Delta T_K}{T_K} \quad (13)$$

$$\Delta T_K = T_K - T_K^0$$

where the superscript zero denotes the absence of salts. Equation 13 can be rewritten as eq.14 from the definition of the activity

$$\ln \frac{X\gamma}{X^0\gamma^0} = \frac{\Delta H_m^\circ}{RT_K^0} \cdot \frac{\Delta T_K}{T_K} \quad (14)$$

where X and γ are the mole fraction and the activity coefficient of the zwitterionic surfactant in micellar phase. In Part I, we discussed the Krafft-point depression phenomenon resulted from the mole fraction change of anionic surfactant in micellar phase. The mole fraction of the zwitterionic surfactant, however, may not vary with added salts because of the very low solubility of salts into the hydrophobic micellar phase. Then, we obtain eq. 15.

$$\ln \frac{\gamma}{\gamma^0} = \frac{\Delta H_m^\circ}{RT_K^0} \cdot \frac{\Delta T_K}{T_K} \quad (15)$$

Assuming that the activity coefficient of the zwitterionic surfactant in the micellar phase decreases with increasing concentration of added salts owing to the electrostatic interaction at the surface of the micelle, $\ln \gamma / \gamma^0$ will be proportional to the square root of the ionic strength of the solution. This may be the reason why the $\Delta T_K / T_K$ values are linearly related to the square root of the salt concentration as shown in Figures 15 and 18. *)

According to the above explanation, the Krafft point of any kinds of zwitterionic surfactant should be depressed by added salts. However, this is not the case as is seen from Figures 16, 17 and 19. Then, the molecular structures of the zwitterionic surfactants classified into the salting-in and non-salting-in group have been examined: and it has been found that the surfactant of salting-in type has more methylene units between nitrogen atom and anionic group than that of non-salting-in type. This result strongly suggests that the governing factor to distinguish between the salting-in type and the non-salting-in type of the surfactant is the distance between positive and negative charge of the surfactant

*) The Krafft point itself is also linearly related to $C_S^{1/2}$ as shown in Figures 16, 17 and 20, since the Krafft-point change upon the addition of salts is small.

molecule. Table 11 shows the charge-charge distance of the zwitterionic surfactant calculated from the known data of bond distances and angles.⁹¹⁻⁹³⁾ It can be understood from Table 11 that the zwitterionic surfactants with the charge-charge distance longer than 0.4-0.5 nm are salted-in. The distance of 0.4-0.5 nm is close to the width of the Stern layer⁹⁴⁻⁹⁵⁾, and may be large enough for the hydrated ions of added salts to enter into the interior of the zwitterions of the surfactant, and interact electrostatically with them at the surface of the micelles. The results of ¹³C-NMR spectra actually indicate that the ions of added salt can more easily come close to the quaternary ammonium group in the case of salting-in type of surfactant (R₁₆DMSPA).

As already mentioned in the previous section, the Krafft point of R₁₈DMSPA in the range of low salt concentrations are the temperatures at which the droplets of liquid crystal dissolve into the water to form micelles. On the other hand, the measured Krafft points in the high salt concentration range are the melting temperatures of the solid agent. The appearance of the inflection in the $\Delta T_K/T_K$ vs. $C_S^{1/2}$ plot for R₁₈DMSPA seems very reasonable from the above point of view. As shown in Table 9, the transition enthalpies of R₁₆DMSPA are almost identical with those of R₁₈DMSPA in the NaCl concentration range above 0.1 M, taking experimental error (+4%) into consideration. The above result

Table 11: Distance between positive and negative charges in zwitterionic surfactant molecules.

Surfactant	Distance/nm	Note
R ₁₈ DMAO	0.133, 0.136 ^{a)}	Non-salting-in
R ₁₆ or R ₁₈ DMCMA	0.31	type
<hr style="border-top: 1px dashed black;"/>		
R ₁₂ CEA	0.45	
R ₁₈ DMCPA	0.55	Salting-in
R ₁₆ or R ₁₈ DMSPA	0.61	type
R ₁₄ DM SA	0.77	

a) The distance of N-O bond is 0.133 nm for l-pyridine oxide²⁰⁾ and 0.136 nm for trimethylamine oxide.²¹⁾

accounts for the similar slope in Figure 5 for R₁₈DMSPA in the high salt concentration range as that for R₁₆DMSPA.

Finally, we have to discuss the Krafft-point elevation of ionic surfactant upon the addition of inorganic salts. The melting-point model is not suitable for this purpose, since the mole fraction of gegenion in ionic micellar phase can be hardly estimated when the added salt is present. The Murray and Hartley's opinion¹⁰⁾ will be used, this time, to explain the Krafft-point elevation of ionic surfactant by added salts.

The activity, a , of the monomer equilibrated with the hydrated solid surfactant can be related to temperature as follows:⁹⁶⁾

$$\partial \ln a / \partial T = \Delta H_s^\circ / RT^2 \quad (16)$$

where ΔH_s° is the standard enthalpy change of solution, T and R are absolute temperature and the gas constant, respectively.

Integrating eq 16 under the condition of temperature independence of ΔH_s° , which is substantiated for R₁₈DMSPA by Figure 21, we obtain

$$-\ln a = (\Delta H_s^\circ / RT) + K \quad (17)$$

where K is an integration constant. The temperature in eq 17 should

be the Krafft point, T_K , when a is the activity at cmc, a_{cmc} , as described previously. Accordingly

$$-\ln a_{cmc} = (\Delta H_S^\circ / RT_K) + K \quad (18)$$

From eq 18, we then derive the next equation.

$$\ln \frac{a_{cmc}}{a_{cmc}^0} = \frac{\Delta H_S^\circ}{R} \left(\frac{1}{T_K^0} - \frac{1}{T_K} \right) = \frac{\Delta H_S^\circ}{RT_K^0} \frac{\Delta T_K}{T_K} \quad (19)$$

$$\Delta T_K = T_K - T_K^0$$

where the superscript zero again denotes the absence of salts. Equation 19 can be rewritten as eq 20 from the definition of the activity,

$$\ln \left(\frac{X\gamma}{X^0\gamma^0} \right)_{\text{at cmc}} = \frac{\Delta H_S^\circ}{RT_K^0} \frac{\Delta T_K}{T_K} \quad (20)$$

where X and γ are the mole fraction and the activity coefficient of the monomer, respectively. The activity coefficient of the zwitterionic monomer is assumed to be constant on addition of salts, as substantiated for R_{18} DMSPA in Figure 21, since the dipole (monomeric zwitterion)-ion interaction is much weaker than the ion-ion interaction. Finally we obtain

$$\ln \frac{\text{cmc}}{\text{cmc}^0} = \frac{\Delta H_S^\circ}{RT_K^0} \frac{\Delta T_K}{T_K} \quad (21)$$

since the mole fraction of the monomer at the cmc is the cmc itself. In Figure 23, the $\ln \text{cmc}/\text{cmc}^0$ is plotted against $\Delta T_K/T_K$ for $R_{12}\text{CEA}$ using the cmc values shown in Table 8. The ΔH_S° value can be calculated from the slope of the straight line to be 101 kJ/mol (= 24.1 kcal/mol) which compares favorably with the reported heat of solution for sodium dodecylsulfonate (21.5 kcal/mol) and sodium tetradecylsulfonate (21.4 kcal/mol).³⁰⁾

In the case of ionic surfactant solutions, the mean activity must be used for the activity in eq 19⁹⁷⁾. This time, we obtain eq 22 instead of eq 20.

$$\ln \left(\frac{X_+ X_-}{X_+^0 X_-^0} \right)_{\text{at cmc}} + 2 \ln \left(\frac{\gamma_{\pm}}{\gamma_{\pm}^0} \right)_{\text{at cmc}} = \frac{\Delta H_S^\circ}{RT_K^0} \frac{\Delta T_K}{T_K} \quad (22)$$

For anionic surfactants, X_- at the cmc is the cmc itself and X_+ is the counterion concentration which is the sum of the cmc and concentration of added salt. Then, eq 22 can be rewritten as follows:

$$\ln \frac{\text{cmc}}{\text{cmc}^0} + \ln \frac{C_s + \text{cmc}}{\text{cmc}^0} + 2 \ln \frac{\gamma_{\pm}}{\gamma_{\pm}^0} = \frac{\Delta H_S^\circ}{RT_K^0} \frac{\Delta T_K}{T_K} \quad (23)$$

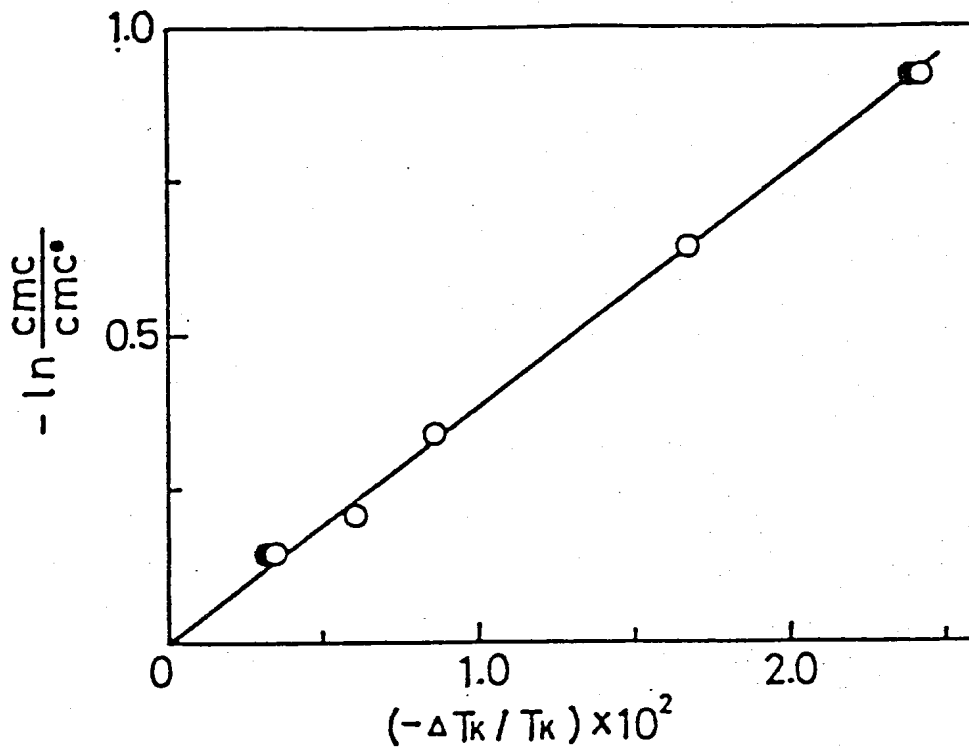


Figure 23. The $\ln cmc/cmc^0$ vs. $\Delta T_K/T_K$ plot for $R_{12}CEA$ in aqueous NaCl solutions. The concentration of $R_{12}CEA$ are 2.0 (\circ) and 5.0 mM (\bullet).

According to the Debye-Hückel theory, the mean activity coefficient for a 1:1 electrolyte can be expressed at 25°C⁹⁸⁾ by

$$\log \gamma_{\pm} = -0.511I^{1/2} = -0.511(C_s + \text{cmc})^{1/2} \quad (24)$$

where I denotes the ionic strength. We can calculate each term of eq 23 for SDS solutions by using the cmc values listed in Table 8. Each term on the left side of eq 23 and their sum is plotted against the $\Delta T_K/T_K$ value in Figure 24. It can be seen from the figure that the Krafft-point elevation of ionic surfactants by added salt is due to the increase of the counterion concentration. Further, it is worth noting that the separate terms of eq 23 are not linearly related, but the sum of them is linear, as expected from eq 23.

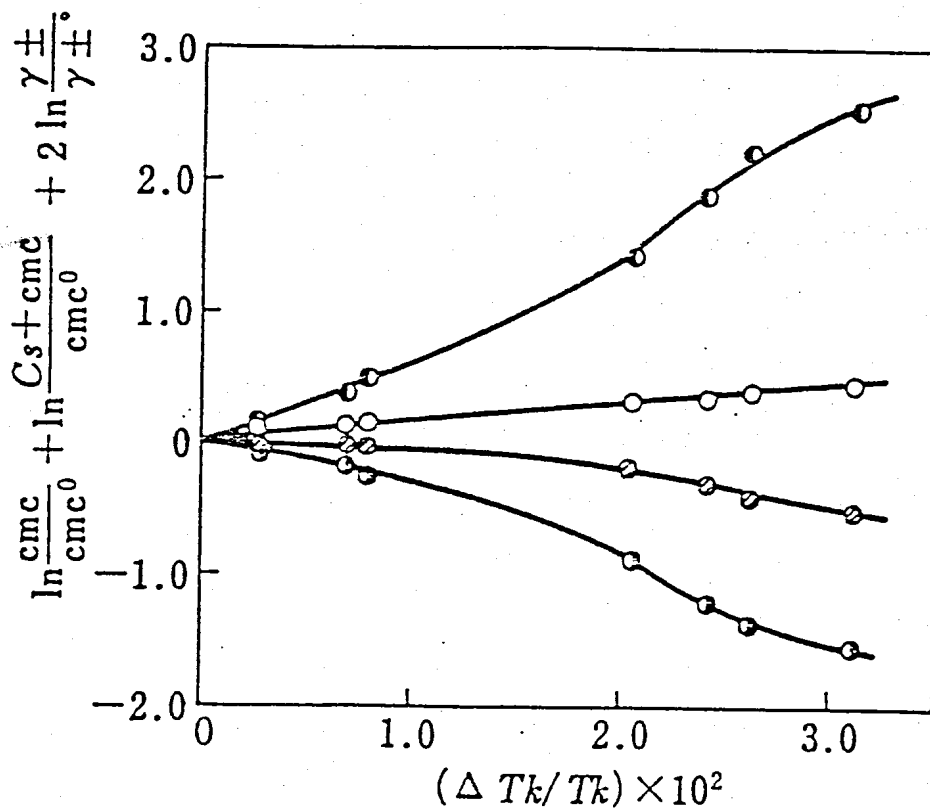


Figure 24. The values of $\ln \text{cmc}/\text{cmc}^0$ (○), $2\ln \gamma_{\pm}/\gamma_{\pm}^0$ (⊙), $\ln (\text{Cs} + \text{cmc}) / \text{cmc}^0$ (⊕), and their sum (○) plotted against $\Delta T_K/T_K$ values for $\text{R}_{12}\text{SO}_4\text{Na}$ in aqueous NaCl solutions.

References

- 1) F. Krafft and H. Wiglow, Ber., 28, 2566 (1895)
- 2) F. Krafft, Ber., 29, 1334 (1896)
- 3) F. Krafft, Ber., 32, 1596 (1899)
- 4) A. Reyhler, Kol. Zeit., 12, 277 (1913)
- 5) J. W. McBain, Trans. Faraday Soc., 9, 99 (1913)
- 6) J. W. McBain and C. S. Salmon, J. Am. Chem. Soc., 42, 426 (1920), and the references cited therein.
- 7) E. R. Jones and C. R. Bury, Phil. Mag., 4, 841 (1927)
- 8) J. Grindley and C. R. Bury, J. Chem. Soc., 679 (1929)
- 9) D. G. Davis and C. R. Bury, J. Chem. Soc., 2263 (1930)
- 10) R. C. Murray and G. S. Hartley, Trans. Faraday Soc., 31, 183 (1935)
- 11) A. Lottermoser and F. Püschel, Koll. Z., 63, 175 (1933)
- 12) R. M. Reed and H. V. Tartar, J. Am. Chem. Soc., 58, 322 (1936)
- 13) H. V. Tartar and K. A. Wright, J. Am. Chem. Soc., 61, 539 (1939)
- 14) H. V. Tartar and R. D. Cadle, J. Phys. Chem., 43, 1173 (1939)
- 15) N. K. Adam and K. G. A. Pankhurst, Trans. Faraday Soc., 42, 523 (1946)
- 16) S. Miyamoto, Bull. Chem. Soc., Jpn., 33, 371 (1960)
- 17) Y Moroi, Yukagaku, 29, 554 (1980)
- 18) K. Shinoda and E. Hutchinson, J. Phys. Chem., 66, 577 (1962)

- 19) A. S. C. Lawrence, Trans. Faraday Soc., 31, 189 (1935)
- 20) A. Lottermoser and F. Stoll, Koll. Z., 63, 49 (1933)
- 21) Y. Moroi, T. Oyama and R. Matsuura, J. Colloid Interface Sci., 60, 103 (1977)
- 22) G. S. Hartley, J. Chem. Soc., 1968 (1938)
- 23) W.D. Harkins, R. W. Mattoon and R. Mittelman, J. Chem. Phys., 15, 763 (1947)
- 24) E. Hutchinson, K. E. Manchester and L. Winslow, J. Phys. Chem., 58, 1124 (1954)
- 25) E. Hutchinson and C. S. Mosher, J. Colloid Sci., 11, 352 (1956)
- 26) E. D. Goddard, C. A. J. Hoeve and G. C. Benson, J. Phys. Chem., 61, 593 (1957)
- 27) K. Shinoda and T. Soda, J. Phys. Chem., 67, 2072, (1963)
- 28) A. Wishnia, J. Phys. Chem., 67, 2079 (1963)
- 29) K. Shigehara, Bull. Chem. Soc., Jpn., 38, 1700 (1965)
- 30) K. Shinoda, S. Hiruta and K. Amaya, J. Colloid Interface Sci., 21, 102 (1966)
- 31) P. Mukerjee, J. Perrin and E. Witzke, J. Pharm. Sci., 58, 1277 (1969)
- 32) F. Tokiwa and K. Tsujii, J. Colloid Interface Sci., 42, 343 (1972)
- 33) G. S. Hartley, "Aqueous Solutions of Paraffin Chain Salts",

Hermann, Paris (1936)

- 34) M. E. L. McBain and E. Hutchinson, "Solubilization and Related Phenomena", Academic Press, New York (1955)
- 35) K. Shinoda, "Colloidal Surfactants" (ed. by K. Shinoda, T. Nakagawa, B. Tamamushi and T. Isemura), p.5, Academic Press, New York (1963)
- 36) P. Mukerjee, Advan. Colloid Interface Sci., 1, 241 (1967)
- 37) P. H. Elworthy, A. T. Florence and C. B. Macfarlane, "Solubilization by Surface Active Agents", p.37, Chapman and Hall Ltd., London (1968)
- 38) C. Tanford, "The Hydrophobic Effect : Formation of Micelles and Biological Membranes" 2nd ed., Chap.6, John Wiley & Sons, New York (1980)
- 39) P. Mukerjee, J. R. Cardinal and N. R. Desai, "Micellization, Solubilization, and Microemulsions" vol.1 (ed. by K. L. Mittal), p.241, Plenum Press, New York (1977)
- 40) K. Shinoda and P. Becher, "Principles of Solution and Solubility", Chap.9, Marcel Dekker Inc., New York (1978)
- 41) H. Nakayama, Bull. Chem. Soc., Jpn., 40, 1592 (1967)
- 42) H. Nakayama and K. Shinoda, Bull. Chem. Soc., Jpn., 40, 1797 (1967)
- 43) M. Hatō and K. Shinoda, Bull. Chem. Soc., Jpn., 46, 3889 (1973)

- 44) K. Shinoda, Y. Minegishi and H. Arai, J. Phys. Chem., 80, 1987 (1976)
- 45) H. Kunieda and K. Shinoda, J. Phys. Chem., 80, 2468 (1976)
- 46) M. Hatō, K. Shinoda and T. Miyagawa, Bull. Chem. Soc., Jpn., 49, 1257 (1976)
- 47) K. Shinoda and T. Hirai, J. Phys. Chem., 81, 1842 (1977)
- 48) H. Nakayama, K. Shinoda and E. Hutchinson, J. Phys. Chem., 70, 3502 (1966)
- 49) K. Shinoda, M. Hatō and T. Hayashi, J. Phys. Chem., 76, 909 (1972)
- 50) M. Hatō and K. Shinoda, J. Phys. Chem., 77, 378 (1973)
- 51) H. Lange and M. J. Schwuger, Kolloid-Z. Z. Polym., 223, 145 (1968)
- 52) M. Murakami, "Dai Yuki Kagaku" vol.1, p.252, Asakura Shoten, Tokyo (1958)
- 53) F. Püschel and C. Kaiser, Chem. Ber., 97, 2917 (1964)
- 54) C. Kaiser and F. Püschel, Chem. Ber., 97, 2926 (1964)
- 55) E. J. Fendler, C. L. Day and J. H. Fendler, J. Phys. Chem., 76, 1460 (1972)
- 56) D. B. Lake and G. L. K. Hoh, J. Am. Oil Chem. Soc., 40, 628 (1963)
- 57) F. Tokiwa and K. Ohki, J. Phys. Chem., 70, 3437 (1966)
- 58) F. Tokiwa and T. Matsumoto, Bull. Chem. Soc., Jpn., 48, 1645 (1975)

- 59) S. Hashimoto, H. Tokuwaka and T. Nagai, *Bunseki Kagaku*, 23, 210 (1974)
- 60) S. Gravsholt, *J. Colloid Interface Sci.*, 57, 575 (1976)
- 61) J. Ulmius, H. Wennerstrom, L. B. Johansson, G. Lindblom and S. Gravsholt, *J. Phys. Chem.*, 83, 2232 (1979)
- 62) K. Tsujii, K. Okahashi and T. Takeuchi, *Yukagaku*, 30, 566 (1981)
- 63) J. K. Weil, A. J. Stirton and E. A. Barr, *J. Am. Oil Chem. Soc.*, 43, 157 (1966)
- 64) J. K. Weil, A. J. Stirton and M. V. Nunez-Ponzoa, *J. Am. Oil Chem. Soc.*, 43, 603 (1966)
- 65) K. Tsujii, N. Saito and T. Takeuchi, *J. Phys. Chem.*, 84, 2287 (1980)
- 66) K. Tsujii, K. Okahashi and T. Takeuchi, *J. Phys. Chem.*, 86, 1437 (1982)
- 67) D. Saul, G. J. T. Tiddy, B. A. Wheeler, P. A. Wheeler and E. Willis, *J. Chem. Soc., Faraday Trans. I*, 70, 163 (1974)
- 68) I. Prigogine and R. Defay, "Chemical Thermodynamics" (translated by M. Seno), Misuzu Shobo, Tokyo, p.366 (1966)
- 69) p.378 in Reference 68.
- 70) Chapter 23 in Reference 68.
- 71) J. G. Kirkwood and I. Oppenheim, "Chemical Thermodynamics" (translated by S. Seki and H. Suga), Tokyo Kagaku Dojin, Tokyo, p.140 (1965)

- 72) W. J. Moore, "Physical Chemistry" 3rd ed., Prentice-Hall Inc., Englewood Cliffs, N. J., p.148 (1962)
- 73) H. Chihara, "Jikken Kagaku Koza" vol.5, Maruzen, Tokyo, p.181 (1958)
- 74) D. N. Rubingh, "Solution Chemistry of Surfactants" (ed. by K. L. Mittal), Plenum Press, New York, p.337 (1979)
- 75) D. G. Kolp, R. G. Laughlin, F. P. Krause and R. E. Zimmerer, J. Phys. Chem., 67, 51 (1963)
- 76) M. J. Rosen, D. Friedman and M. Gross, J. Phys. Chem., 68, 3219 (1964)
- 77) A. Nakamura and M. Muramatsu, J. Colloid Interface Sci., 62, 165 (1977)
- 78) K. Tajima, A. Nakamura and T. Tsutsui, Bull. Chem. Soc., Jpn., 52, 2060 (1979)
- 79) R. C. Murray, Trans. Faraday Soc., 31, 199 (1935)
- 80) M. J. Schwuger, Kolloid-Z. Z. Polym., 233, 979 (1969)
- 81) H. Schott and S. K. Han, J. Pharm. Sci., 65, 979 (1976)
- 82) K. Tsujii and J. Mino, J. Phys. Chem., 82, 1610 (1978)
- 83) K. Tsujii and T. Takeuchi, Yukagaku, 30, 495 (1981)
- 84) K. Hachiya, N. Takaishi, Y. Inamoto and K. Tsujii, Submitted to Japan Patent.
- 85) T. Okumura, K. Tajima and T. Sasaki, Bull. Chem. Soc., Jpn., 47, 1067 (1974)
- 86) F. Tokiwa and K. Ohki, J. Phys. Chem., 71, 1824 (1967)

- 87) F. B. Rosevear, J. Am. Oil Chem. Soc., 31, 628 (1954)
- 88) F. B. Rosevear, J. Soc. Cosmet. Chem., 19, 581 (1968)
- 89) A. Saupe, J. Colloid Interface Sci., 58, 549 (1977)
- 90) D. Demus and L. Richter, "Textures of Liquid Crystals", Verlag Chemie, New York (1978)
- 91) L. Pauling, "The nature of chemical bond" (translated by M. Koizumi), Kyoritsu Shuppan, Tokyo (1975)
- 92) R. A. Abramovitch and E. M. Smith, "Heterocyclic Compounds" vol.14, Part 2, John Wiley & Sons, New York (1974), p.31
- 93) S. Oae, "Yuki Io Kagobutsu", Kagaku Dojin, Kyoto (1969), p.297
- 94) D. Stigter, J. Colloid Interface Sci., 23, 379 (1967)
- 95) D. Stigter, J. Phys. Chem., 79, 1008 (1975)
- 96) Chapters 18 and 22 in Reference 68
- 97) K. Shirahama, Bull. Chem. Soc., Jpn., 47, 3165 (1974)
- 98) G. L. Lewis and M. Randall "Thermodynamics" revised by K. S. Pitzer and L. Brewer, 2nd ed., McGraw-Hill, New York, P.338 (1961)

Acknowledgments

The author wishes to express his sincere thanks to Professors Hiroshi Suga, Hideaki Chihara, Yoshimasa Kyogoku and Toshio Takagi of Osaka University, and Professor Syūzō Seki of Kwansai Gakuin University, and Drs. Fumikatsu Tokiwa, Kunihiko Nagase, Masahiro Saito and Takashi Takeuchi of Kao Corporation for their encouragements and kind guidances for this work. He also thanks many of his colleagues of Wakayama, Tokyo and Tochigi Research Laboratories of Kao Corporation for their help in sample preparations and a lot of useful and kind discussions and comments. He finally expresses his gratitude greatly to Dr. Yoshio Maruta, the president of Kao Corporation, for his permission to publish this paper.